SIAM J. SCI. COMPUT.
Vol. 41, No. 3, pp. B545–B575

UNCERTAINTY QUANTIFICATION FOR MULTIGROUP DIFFUSION EQUATIONS USING SPARSE TENSOR APPROXIMATIONS*

CONSUELO FUENZALIDA†, CARLOS JEREZ-HANCKES‡, AND RYAN G. MCCLARREN§

Abstract. We develop a novel method to compute first and second order statistical moments of the neutron kinetic density inside a nuclear system by solving the energy-dependent neutron diffusion equation. Randomness comes from the lack of precise knowledge of external sources as well as of the interaction parameters, known as cross sections. Thus, the density is itself a random variable. As Monte Carlo simulations entail intense computational work, we are interested in deterministic approaches to quantify uncertainties. By assuming as given the first and second statistical moments of the excitation terms, a sparse tensor finite element approximation of the first two statistical moments of the dependent variables for each energy group can be efficiently computed in one run. Numerical experiments provided validate our derived convergence rates and point to further research avenues.

Key words. multigroup diffusion equation, uncertainty quantification, sparse tensor approximation, finite element method

AMS subject classifications. 82D75, 65M60, 35R60, 65C50

DOI. 10.1137/18M1185995

1. Introduction.

The general problem of particle transport can be applied to a variety of situations from rarefied gas dynamics for aircraft in the upper atmosphere to charged particle transport in space environments, as well as nuclear reactions in energy systems [25] and radiative transfer in the atmosphere [31]. While there are a number of developed techniques for solving these problems, the question of how uncertainties in the simulation inputs affect the predictions remains a challenging task both numerically and theoretically [29, 30, 27, 18, 13].

We aim to tackle high-dimensional uncertainties in particle transport problems by considering steady-state multigroup diffusion equations. This model is widely used in nuclear reactor theory for solving the phase-space distribution of neutrons in a system where neutron-nucleus reactions occur, despite its limitations for specific physical situations [33, 23]. Of particular interest for nuclear engineers is the eigenvalue problem of computing the neutron fission chain reaction, or so-called criticality parameters, for which first existence theorems were provided by Habetler and Martino [10], and numerous computational schemes have been developed [11, 32, 20]. Numerically, the criticality problem is an eigenvalue problem that can be solved via the standard finite element method (FEM) built over general triangular meshes [17, 41]. Based on this computational method, we will provide an efficient way to compute statistical

*Submitted to the journal's Computational Methods in Science and Engineering section May 7, 2018; accepted for publication (in revised form) April 3, 2019; published electronically June 20, 2019.
http://www.siam.org/journals/sisc/41-3/M118599.html

Funding: This work was partially supported by the Corfo 2030 Seed Fund Program TAMU-PUC 201603 and Fondecyt Regular 1171491.

†School of Engineering, Pontificia Universidad Católica de Chile, Santiago, Chile (mcfuenzalida@uc.cl).

‡Faculty of Engineering and Sciences, Universidad Adolfo Ibañez, Santiago, Chile (carlos.jerez@uai.cl).

§Department of Aerospace and Mechanical Engineering, College of Engineering, University of Notre Dame, Notre Dame, IN 46556 (rmcclarr@nd.edu).

moments for solutions subject to uncertainty in the sources. Nonetheless, we will not address the associated eigenvalue problem. Rather, we focus on the forward problem where we solve for the distribution of neutrons given a source. Such problems are important in radiation protection/shielding and nuclear hydrocarbon exploration/production.

The standard method of choice for operator equations with uncertain input data subject to noisy observation data is the Monte Carlo (MC) algorithm and its variants: Markov chain MC, ensemble Kalman filter, or sequential MC, to name by a few (cf. [7] and references therein). Typically, MC-based algorithms converge slowly, as $\mathcal{O}(M^{-1/2})$, for estimates of distribution moments, subject to M numerical solutions of the operator equation under consideration [26]. Despite this slow convergence, MC algorithms are free from the *curse of dimensionality*, i.e., the convergence rate $\mathcal{O}(M^{-1/2})$ is ensured independently of the number of parameters in the model describing the uncertainty. An alternative to MC methods is deterministic approaches that directly compute properties of the statistical distribution. Nevertheless, when the problem possesses *distributed random input data*, such as domain geometry, heterogeneous material properties, etc., these deterministic representations do suffer from the curse of dimensionality and the amount of work required to compute the representation of the solution increases exponentially in the number of dimensions. Example deterministic techniques are Karhúnen–Loève, Fourier, or wavelet expansions of shapes and material properties. The deterministic representations lead to the mathematical problem of *high-dimensional interpolation and integration*, accompanied by numerical techniques such as polynomial chaos, model order reduction, or stochastic FEM [2, 8].

In this work, we present a novel combination of sparse, tensorized FEM discretizations with computational efficient techniques in the context of uncertainty estimation in multigroup neutron diffusion. This constitutes a significant extension of the ideas developed by Schwab et al. [40, 16, 21] to efficiently approximate statistical moments of the radiative transport solutions due to uncertainty in the sources. Broadly speaking, if the operators are deterministic, statistical moments can be taken directly on the unknowns and sources, thereby turning the problem into a tensorized deterministic one. The only requirement is knowledge of the sources' statistical moments. Though the problem considered is of higher dimension, the associated tensorized systems can be numerically solved without ever forming the tensor form matrix resulting from standard FEM. Moreover, by sparsifying the tensor systems, computational work and memory grow only polylogarithmically for increasing degrees of freedom. Application of sparse tensor methods for purely deterministic transport equations was carried out by Schwab et al. [34, 35] reducing the number of degrees associated to angular and spatial directions. To reduce computational complexity, the combination technique developed by Harbrecht, Peters, and Siebenmorgen [15] is employed.

To our knowledge, the extension of tensor techniques to solve problems set in Cartesian product spaces has never been performed, and as we will see, these new structural conditions constitute a major challenge to the method. Indeed, both full and sparse tensor approaches suffer from the deterioration of condition numbers due to the tensor product structure of the bilinear forms. This phenomenon, dubbed "double conditioning," is due to the squaring of the associated Galerkin matrix condition number (cf. Lemma 5.11). Moreover, this issue is enhanced by the forward block elimination scheme employed to sequentially solve the linear systems for each energy group. Indeed, standard FEM implementations lead to an error build-up arising from forward substitution for consecutive energy levels: as the number of energy groups grows, convergence worsens (cf. Theorem 5.7 and Remark 5.8). In this sense, our findings clearly show these shortcomings and tackling them is part of our current research efforts.

The article is structured as follows. Section 2 introduces our model problem, with sections 3 and 4 discussing variational formulations for the deterministic and stochastic versions, respectively. Of particular interest is the well-posedness of the problem and deterministic computation of statistical problems. Section 5 presents the numerical discretization scheme used along with convergence rates. Computational experiments are developed in sections 6 and 7 for homogeneous and nonhomogeneous random sources, respectively, validating our theoretical claims. Finally, conclusions and future research lines are sketeched in section 8, with an appendix provided for completeness.

2. Preliminaries.

2.1. Notation. Throughout, scalar quantities will be denoted by normal fonts and vector ones by boldface. We write $\mathbb{N}$ for the set of natural numbers, $\mathbb{N}_0 := \mathbb{N} \cup \{0\}$, $\mathbb{R}$ the set of real numbers.

Let $O \subset \mathbb{R}^d$, $d = 1, 2$, be an open and Lipschitz domain. For $k \in \mathbb{N}_0$, $\mathcal{C}^k(O)$ represents the space of continuous functions whose k derivatives are also continuous. The class of p-integrable functions over O is $L^p(O)$ for $p \geq 1$. We denote the standard Sobolev spaces [37] by $H^s(O)$ for $s \in \mathbb{R}$, with $H^0(O) \equiv L^2(O)$, dual $\widetilde{H}^{-s}(O)$, and norms denoted by $\|\cdot\|_{H^s(O)}$. Duality pairings are denoted by $\langle \cdot, \cdot \rangle$ with subscripts indicating the domain of involved functional spaces, if it is not clear from the context. Similarly, inner products are written as $(\cdot, \cdot)$, only requiring integration domains as subscript.

2.2. Multigroup diffusion equation and its parameters. We will work in two-dimensional physical domain though the whole program can directly be extended to three dimensions.

Let $\mathcal{D} \subset \mathbb{R}^2$ be an open bounded Lipschitz domain, and let the energy range $[\mathcal{E}_0, \mathcal{E}_{N_E}]$ with $\mathcal{E}_{N_E} > \mathcal{E}_0 \geq 0$ be partitioned into N_E nonoverlapping intervals $[\mathcal{E}_{N_E-e}, \mathcal{E}_{Ne-e+1}]$; the interval $[\mathcal{E}_{N_E-e}, \mathcal{E}_{N_E-e+1}]$ is called *energy group* e, with $e = 1, \ldots, N_E$. The migration of neutrons through a material medium can be modeled using the multigroup neutron diffusion equation [3, 36],

$$
\begin{aligned}
(1) \qquad & -\nabla \cdot D^{(e)}(\mathbf{x}) \nabla u^{(e)}(\mathbf{x}) + \sigma_r^{(e)}(\mathbf{x}) u^{(e)}(\mathbf{x}) \\
& \quad - \sum_{\hat{e} \neq e} \sigma_s^{(\hat{e} \to e)}(\mathbf{x}) u^{(\hat{e})}(\mathbf{x}) = f^{(e)}(\mathbf{x}) \quad \forall e = 1, \ldots, N_E,
\end{aligned}
$$

wherein $u^{(e)}(\mathbf{x})$ is the neutron flux integrated over an energy range $[\mathcal{E}_{N_E-e}, \mathcal{E}_{N_E-e+1}]$, and is interpreted as the number density of neutrons at $\mathbf{x}$ multiplied by an average neutron speed. The removal cross section $\sigma_r^{(e)}$ for group e is given by

$$
\sigma_r^{(e)} = \sigma_a^{(e)} + \sum_{\hat{e} \neq e} \sigma_s^{(e \to \hat{e})},
$$

where $\sigma_a^{(e)}$ is the absorption cross section for energy group e at the position $\mathbf{x} \in \mathcal{D}$ with units of inverse length, and $\sigma_s^{(\hat{e} \to e)}$ is the scattering cross section from energy group $\hat{e}$ to e at position $\mathbf{x} \in \mathcal{D}$. $D^{(e)}$ is the piecewise-constant energy group diffusion coefficient with units of length. Finally, $f^{(e)}$ is the prescribed source (in units of number density per unit time) of neutrons into energy group e at position $\mathbf{x}$.

Assumption 2.1. In the following, we will assume cross sections $\sigma_a^{(e)}$, $\sigma_s^{(\hat{e}\to e)}$ and diffusion coefficients to lie in $L^\infty(\mathcal{D})$ and be nonnegative measurable functions satisfying the following *subcriticality conditions* [5, eqn. 9(a)–(c)]:

$$0 < \sigma_0 \le \sigma_r^{(e)} \le \sigma_\infty, \tag{2}$$

$$\sigma_a^{(e)} + \sum_{e=1}^{N_E} \sigma_s^{(e\to\hat{e})} - \sum_{\hat{e}=1}^{N_E} \sigma_s^{(\hat{e}\to e)} \ge \alpha > 0, \tag{3}$$

$$\sigma_a^{(e)} \ge \alpha > 0, \tag{4}$$

for $\hat{e}, e = 1, \dots, N_E$. These conditions imply that physically there can be no neutron chain reactions that do not end in finite time.

2.3. Boundary and interface conditions. Let $\mathcal{D} \subset \mathbb{R}^2$ be any open Lipschitz domain. We denote the standard Dirichlet and Neumann traces by γ_{D} and γ_{N}, respectively, defined over functions f in $\mathcal{C}^\infty(\mathcal{D})$ as

$$(\gamma_{\mathrm{D}} f)(\mathbf{x}) := \lim_{\tilde{\mathbf{x}}\in\mathcal{D}\to\mathbf{x}\in\partial\mathcal{D}} f(\tilde{\mathbf{x}}), \qquad (\gamma_{\mathrm{N}} f)(\mathbf{x}) := \lim_{\tilde{\mathbf{x}}\in\mathcal{D}\to\mathbf{x}\in\partial\mathcal{D}} \hat{\mathbf{n}}\cdot\nabla f(\tilde{\mathbf{x}}),$$

where $\mathbf{n}$ is the outward normal to the boundary $\partial\mathcal{D}$ and with known extensions [37] $\gamma_{\mathrm{D}} : H^1(\mathcal{D}) \to H^{\frac{1}{2}}(\partial\mathcal{D})$ and $\gamma_{\mathrm{N}} : H^1(\mathcal{D}) \to H^{-\frac{1}{2}}(\partial\mathcal{D})$.

On the boundary $\partial\mathcal{D}$, we will employ the so-called Marshak boundary conditions, which are mixed or Robin boundary conditions approximating no neutrons entering the domain [6], for each energy group $e = 1, \dots, N_E$,

$$\gamma_{\mathrm{N}} u^{(e)}(\mathbf{x}) + \frac{1}{2D^{(e)}(\mathbf{x})}\gamma_{\mathrm{D}} u^{(e)}(\mathbf{x}) = 0 \quad \forall\ \mathbf{x} \in \partial\mathcal{D}. \tag{5}$$

If $\mathcal{D}$ is made up of different disjoint $N_{dom} \in \mathbb{N}$ subdomains, e.g., $\overline{\mathcal{D}} = \bigcup_{i=1}^{N_{dom}} \overline{\mathcal{D}}_i$, with $\mathcal{D}_i \cap \mathcal{D}_j = \emptyset$, for $i \neq j$, one may be required to state interface conditions. Without loss of generality, let us assume that $\mathcal{D}$ is composed of two such disjoint subdomains such that $\overline{\partial\mathcal{D}}_1 \cap \overline{\partial\mathcal{D}}_2 \neq \emptyset$ and that $u^{(e)}$ is a solution of (1). Then, for $u_i^{(e)} := u^{(e)}|_{\mathcal{D}_i}$, $i = 1, 2$, being restrictions of the neutron flux over each subdomain, transmission conditions are given by [9, sect. 2.5]:

$$\gamma_{\mathrm{D}}^1 u_1^{(e)} = \gamma_{\mathrm{D}}^2 u_2^{(e)} \qquad \text{on } \partial\mathcal{D}_1 \cap \partial\mathcal{D}_2, \tag{6a}$$

$$D_1^{(e)}\gamma_{\mathrm{N}}^1 u_1^{(e)} = D_2^{(e)}\gamma_{\mathrm{N}}^2 u_2^{(e)} \quad \text{on } \partial\mathcal{D}_1 \cap \partial\mathcal{D}_2, \tag{6b}$$

where $D_i^{(e)}$ is the constant value of the diffusion coefficient $D^{(e)}(\mathbf{x})$ inside the subdomain $\mathcal{D}_i$, $i = 1, 2$, respectively, and γ_{D}^i, γ_{N}^i, denote the corresponding trace operators.

3. Continuous deterministic model. In what follows, we formally state the deterministic model problem of steady-state neutron flux to be studied. Our setting will be that of H^1-spaces as in [5]; we also recall conditions for uniqueness and existence of solutions.

3.1. Deterministic strong formulation. For each energy group, let us define two operators:

$$\mathcal{A}^{(e)} u^{(e)} := \left(-\nabla\cdot D^{(e)}\nabla + \sigma_r^{(e)}\right) u^{(e)}, \tag{7}$$

$$\mathcal{B}^{(e\hat{e})} u^{(\hat{e})} := -\sigma_s^{(\hat{e}\to e)} u^{(\hat{e})}, \tag{8}$$

with $e, \hat{e} = 1, \ldots, N_E$. Though coefficients and cross sections may vary inside $\mathcal{D}$, our hypotheses allow us to conclude that both $\mathcal{A}^{(e)} : H^1(\mathcal{D}) \to \widetilde{H}^{-1}(\mathcal{D})$ and $\mathcal{B}^{(e\hat{e})} : H^1(\mathcal{D}) \to H^1(\mathcal{D})$ are linear and continuous. Then, the strong formulation for the multigroup diffusion equation problem reads as follows.

Problem 3.1. For all $e = 1, \ldots, N_E$, let $f^{(e)} \in \widetilde{H}^{-1}(\mathcal{D})$. We seek $u^{(e)} \in H^1(\mathcal{D})$ such that

$$\mathcal{A}^{(e)} u^{(e)} + \sum_{\hat{e} \neq e} \mathcal{B}^{(e\hat{e})} u^{(\hat{e})} = f^{(e)} \quad \text{in } \mathcal{D}, \tag{9a}$$

$$\gamma_{\mathrm{N}} u^{(e)} + \frac{1}{2D^{(e)}} \gamma_{\mathrm{D}} u^{(e)} = 0 \quad \text{on } \partial\mathcal{D}. \tag{9b}$$

Furthermore, we can define operator matrices $\mathbb{A} : [H^1(\mathcal{D})]^{N_E} \to [\widetilde{H}^{-1}(\mathcal{D})]^{N_E}$ and $\mathbb{B} : [H^1(\mathcal{D})]^{N_E} \to [H^1(\mathcal{D})]^{N_E} \subset [\widetilde{H}^{-1}(\mathcal{D})]^{N_E}$ containing operators for all energy groups:

$$\mathbb{A} := \operatorname{diag}(\mathcal{A}^{(1)}, \ldots, \mathcal{A}^{(N_E)}), \quad \mathbb{B} := \begin{bmatrix} 0 & \mathcal{B}^{(12)} & \cdots & \mathcal{B}^{(1N_E)} \\ \mathcal{B}^{(21)} & 0 & \cdots & \vdots \\ \vdots & \vdots & \ddots & \vdots \\ \mathcal{B}^{(N_E 1)} & \mathcal{B}^{(N_E 2)} & \cdots & 0 \end{bmatrix}. \tag{10}$$

Defining $\mathbb{D} := (\mathbb{A} + \mathbb{B})$ and setting $\mathbf{f} = (f^{(1)}, \ldots, f^{(N_E)})$ in $[\widetilde{H}^{-1}(\mathcal{D})]^{N_E}$, (9a) and (9b) can be equivalently written as

$$\mathbb{D}(\mathbf{x})\mathbf{u}(\mathbf{x}) = \mathbf{f}(\mathbf{x}) \quad \forall\, \mathbf{x} \in \mathcal{D}, \tag{11a}$$

$$\gamma_{\mathrm{N}} \mathbf{u}(\mathbf{x}) + \frac{1}{2} \mathsf{D}^{-1}(\mathbf{x}) \gamma_{\mathrm{D}} \mathbf{u}(\mathbf{x}) = \mathbf{0} \qquad \forall\, \mathbf{x} \in \partial\mathcal{D}, \tag{11b}$$

where $\mathbf{u} = \left(u^{(1)}, \ldots, u^{(N_E)}\right)$ in $[H^1(\mathcal{D})]^{N_E}$ and we have defined the diffusion coefficient matrix:

$$\mathsf{D}(\mathbf{x}) := \operatorname{diag}\left(D^{(1)}(\mathbf{x}), \ldots, D^{(N_E)}(\mathbf{x})\right) \quad \forall\, \mathbf{x} \in \mathcal{D}.$$

3.2. Deterministic variational formulation. For $e = 1, \ldots, N_E$, the variational form of Problem 3.1 can be written as

$$\mathsf{a}^{(e)}(u^{(e)}, v) + \sum_{\hat{e} \neq e} \mathsf{b}^{(\hat{e}e)}(u^{(e)}, v) = \left\langle f^{(e)}, v \right\rangle_{\mathcal{D}} \quad \forall\, v \in H^1(\mathcal{D}), \tag{12}$$

wherein the bilinear forms $\mathsf{a}^{(e)}(\cdot,\cdot)$ and $\mathsf{b}^{(\hat{e}e)}(\cdot,\cdot)$ are induced by the aforementioned operators as

$$\begin{aligned} \mathsf{a}^{(e)}(u^{(e)}, v) &:= \int_D D^{(e)}(\mathbf{x}) \nabla u^{(e)}(\mathbf{x}) \cdot \nabla v(\mathbf{x}) d\mathbf{x} + \frac{1}{2} \int_{\partial\mathcal{D}} \gamma_{\mathrm{D}} u^{(e)}(\mathbf{x}) \gamma_{\mathrm{D}} v(\mathbf{x}) d\mathbf{x} \\ &\quad + \int_D \sigma_r^{(e)}(\mathbf{x}) u(\mathbf{x}) v(\mathbf{x}) d\mathbf{x}, \\ \mathsf{b}^{(\hat{e}e)}(u^{(e)}, v) &:= -\int_D \sigma_s^{(\hat{e} \to e)}(\mathbf{x}) u^{(e)}(\mathbf{x}) v(\mathbf{x}) d\mathbf{x} \end{aligned}$$

by using integration-by-parts and the boundary condition (9b). Clearly, both forms are continuous and bounded. However, it is less obvious to see that (12) is well posed.

LEMMA 3.2 (Theorem 4 in [5]). *Assume that the* $u^{(\hat{e})} \in H^1(\mathcal{D})$ *are given for* $\hat{e} \neq e$. *For* $f^{(e)} \in L^2(\mathcal{D})$ *and under subcriticality conditions* (2)–(4), *problem* (12) *has a unique solution* $u^{(e)} \in H^1(\mathcal{D})$ *for each* $e = 1, \dots, N_E$.

The proof is based on the Fredholm alternative [37, Thm. 3.35] and on the injectivity of the bilinear form for the case of subcritical conditions. In particular, the coercivity estimates arise by shifting the compact pertubation provided by the substraction of mass terms multiplied by $\sigma_r^{(e)}$ and $\sigma_s^{(\hat{e}\to e)}$ and the compact embedding $H^1(\mathcal{D}) \hookrightarrow L^2(\mathcal{D})$ (cf. [5, 12] and [37]).

Similarly, we can state the variational formulation for the entire multigroup diffusion system (11a) with boundary conditions (11b) by considering the bilinear form

$$\mathsf{d}(\mathbf{u},\mathbf{v}) := \langle \mathbb{D}\,\mathbf{u},\mathbf{v}\rangle_{\mathcal{D}} = \sum_{e=1}^{N_E} \mathsf{a}^{(e)}(u^{(e)}, v^{(e)}) + f \sum_{e=1}^{N_E} \sum_{\hat{e}\neq e} \mathsf{b}^{(\hat{e}e)}(u^{(e)}, v^{(e)}) \tag{13}$$

for $\mathbf{u}$ and $\mathbf{v}$ in $[H^1(\mathcal{D})]^{N_E}$. The above is derived by interpreting the duality pairing over the Cartesian product space $[H^1(\mathcal{D})]^{N_E}$ as the sum over all N_E individual $H^1(\mathcal{D})$-pairings and using the integration-by-parts formula.

Problem 3.3. Let $\mathbf{f} \in [\widetilde{H}^{-1}(\mathcal{D})]^{N_E}$. Find $\mathbf{u} \in [H^1(\mathcal{D})]^{N_E}$ such that

$$\mathsf{d}(\mathbf{u},\mathbf{v}) = \langle \mathbf{f},\mathbf{v}\rangle_{\mathcal{D}} \quad \forall\ \mathbf{v} \in [H^1(\mathcal{D})]^{N_E}, \tag{14}$$

where the source term is just the sum of individual dual products $\left\langle f^{(e)}, v^{(e)}\right\rangle_{\mathcal{D}}$ over each energy group.

COROLLARY 3.4 (Theorem 7 in [5]). *Assume* $\mathbf{f} \in [\widetilde{H}^{-1}(\mathcal{D})]^{N_E}$. *Then, Problem* 3.3 *has a unique solution* $\mathbf{u} \in [H^1(\mathcal{D})]^{N_E}$. *Moreover, the operator* $\mathbb{D}$ *is boundedly invertible.*

Assumption 3.5. In order to obtain convergence estimates, we will later assume that there exist bounded mappings $\mathbb{D}^{-1}$ from $[\widetilde{H}^{-1+s}(\mathcal{D})]^{N_E}$ to $[H^{1+s}(\mathcal{D})]^{N_E}$, for $0 \leq s \leq s_0$, with s_0 depending on the domain regularity and smoothness of parameters and sources. We will not elaborate on this and point out the relevant work by Stewart [38, 39].

4. Continuous stochastic model.

In (1), both source and parameters are deterministic. However, in reality, sources are composed of materials that release neutrons, involving epistemic and aleatoric uncertainties, as measurements are not accurate and neutrons behave differently each time the experiment is made. Similarly, cross sections' uncertainties also suffer of such types of randomness [42].

4.1. Abstract theory.

In order to quantify uncertainty effects, we introduce parts of the theory presented in [40, 21]. Let $(\Omega, \mathcal{F}, \mathbb{P})$ be a probability space, where, as is customary, Ω denotes the set of all elementary events, $\mathcal{F}$ the associated σ-algebra, and $\mathbb{P}$ a probability measure. We define a random field g with values in a separable Hilbert space X as a strongly measurable mapping $g : \Omega \to X$ which maps events $E \in \mathcal{F}$ to Borel sets in X. This induces a measure $\widetilde{\mathbb{P}}$ on X.

For $k \in \mathbb{N}$, the random variable $g : \Omega \to X$ lies in the Bochner integrable space $L^k(\Omega, \mathbb{P}; X)$ if $\omega \mapsto \|g(\omega)\|_X^k$ is measurable and integrable, satisfying

$$\|g\|^k_{L^k(\Omega,\mathbb{P};X)} := \int_\Omega \|g(\omega)\|_X^k \,\mathrm{d}\mathbb{P}(\omega) < \infty.$$

If $g \in L^1(\Omega, \mathbb{P}; X)$, the expectation

$$\mathbb{E}[g] \ := \ \int_\Omega g(\omega) \mathrm{d}\mathbb{P}(\omega) \ \in \ X \tag{15}$$

exists as a Bochner integral with

$$\|\mathbb{E}[g]\|_X \ \leq \ \|g\|_{L^1(\Omega,\mathbb{P};X)} \,. \tag{16}$$

Let B belong to $\mathcal{L}(X, Y)$, the space of linear continuous mappings from X to Y. For a random variable g in $L^k(\Omega, \mathbb{P}; X)$ one constructs another random variable $h(\omega) = \mathsf{B}g(\omega) \in L^k(\Omega, \mathbb{P}; Y)$ satisfying

$$\|\mathsf{B}g\|_{L^k(\Omega,\mathbb{P};Y)} \ \leq \ \|g\|_{L^k(\Omega,\mathbb{P};X)} \,. \tag{17}$$

Furthermore,

$$\mathsf{B} \int_\Omega g(\omega) \mathrm{d}\mathbb{P}(\omega) \ = \ \int_\Omega \mathsf{B}g(\omega) \mathrm{d}\mathbb{P}(\omega) \,. \tag{18}$$

For $k \in \mathbb{N}$, the k-fold Hilbertian tensor product space is defined as

$$X^{(k)} \ := \ \underbrace{X \otimes \cdots \otimes X}_{k\text{-times}} \tag{19}$$

equipped with the natural norm $\|\cdot\|_{X^{(k)}}$, which is a cross-norm, i.e.,

$$\|g_1 \otimes \cdots \otimes g_k\|_{X^{(k)}} \ = \ \|g_1\|_X \cdots \|g_k\|_X \ , \tag{20}$$

for all $g_1, \ldots, g_k$ in X. Taking $\mathsf{B} \in \mathcal{L}(X, Y)$, there is a unique linear, continuous tensor product operator:

$$\mathsf{B}^{(k)} \ := \ \underbrace{\mathsf{B} \otimes \cdots \otimes \mathsf{B}}_{k\text{-times}} \ \in \ \mathcal{L}(X^{(k)}, Y^{(k)}) \,. \tag{21}$$

For a random field $u \in L^k(\Omega, \mathbb{P}; X)$, let the k-fold simple tensor product $u^{(k)}(\omega) := u(\omega) \otimes \cdots \otimes u(\omega)$. Then, $u^{(k)} \in L^1(\Omega, \mathbb{P}; X^{(k)})$. For $u \in L^k(\Omega, \mathbb{P}; X)$ with finite $k \in \mathbb{N}$, the kth moment of $u(\omega)$ is defined by

$$\mathcal{M}^k u \ = \ \mathbb{E}\big[\underbrace{u \otimes \cdots \otimes u}_{k\text{-times}}\big] \ = \ \int_{\omega\in\Omega} \underbrace{u(\omega) \otimes \cdots \otimes u(\omega)}_{k\text{-times}} \mathrm{d}\mathbb{P}(\omega) \,. \tag{22}$$

Nonetheless, in the present work we will just focus on first and second order moments, i.e., $k = 1, 2$. Observe that, for $k \in \mathbb{N}$, we denote by $X^k = X \times \cdots \times X$ the k-fold Cartesian product of X, with graph norm given by the sum of k components. This is different from the k-fold tensor product $X^{(k)}$ in (19).

The next result justifies deterministic computations of first and second order statistical moments.

Proposition 4.1 (Theorem 6.1 in [21]). *Assume given* $\mathsf{A} \in \mathcal{L}(X, Z)$, $\mathsf{B} \in \mathcal{L}(Y, Z)$ *for three Hilbert spaces* X, Y, Z, *with* A *boundedly invertible. Then, for* $f \in L^2(\Omega, \mathbb{P}; Y)$, *the solution of the stochastic operator equation*

$$\mathsf{A}u(\omega) = \mathsf{B}f(\omega) \tag{23}$$

admits a unique solution $u \in L^2(\Omega, \mathbb{P}; X)$ *whose first and second moments,* $\mathbb{E}[u] \in X$ *and* $\mathcal{M}^2 u := \mathbb{E}[u \otimes u] \in X^{(2)}$*, respectively, uniquely solve the associated deteministic equations:*

$$\mathsf{A}\mathbb{E}[u] = \mathsf{B}\mathbb{E}[f] \quad in \quad Z \tag{24}$$

and

$$(\mathsf{A} \otimes \mathsf{A}) u^{(2)} = (\mathsf{B} \otimes \mathsf{B}) \mathcal{M}^2 f \quad in \quad Z^{(2)}\ , \tag{25}$$

where $\mathcal{M}^2 f := \mathbb{E}[f \otimes f] \in Y^{(2)}$*.*

4.2. First statistical moment. We now consider stochastic sources $f^{(e)}(\mathbf{x}, \omega)$ with $\omega \in (\Omega, \mathcal{F}, \mathbb{P})$. As in section 3, we state the strong and variational formulations for the first statistical moment problem. As shorthand, we identify for brevity $X^s \equiv [H^{1+s}(\mathcal{D})]^{N_E}$ and $Z^s \equiv [\widetilde{H}^{-1+s}(\mathcal{D})]^{N_E}$, with $X \equiv X^0$ and $Z \equiv Z^0$ hereafter.

4.2.1. Strong formulation. Assuming sources to be stochastic while keeping physical parameters deterministic, we rewrite Problem 3.1 as follows. Let $f^{(e)} \in L^1(\Omega, \mathbb{P}, \widetilde{H}^{-1}(\mathcal{D}))$ for $e = 1, \ldots, N_E$. For each realization $\omega \in (\Omega, \mathcal{F}, \mathbb{P})$, we seek $u^{(e)} \in L^1(\Omega, \mathbb{P}, H^1(\mathcal{D}))$ such that

$$\mathcal{A}^{(e)} u^{(e)}(\omega) + \sum_{\hat{e} \neq e} \mathcal{B}^{(e\hat{e})} u^{(\hat{e})}(\omega) = f^{(e)}(\omega) \quad \text{in } \mathcal{D}, \tag{26a}$$

$$\gamma_{\mathrm{N}} u^{(e)}(\omega) + \frac{1}{2D^{(e)}} \gamma_{\mathrm{D}} u^{(e)}(\omega) = 0 \qquad \text{on } \partial\mathcal{D} \tag{26b}$$

for $e = 1, \ldots, N_E$. Equivalently, and as before, (26a) and (26b) can be summarized as

$$\mathbb{D}(\mathbf{x}) \mathbf{u}(\mathbf{x}, \omega) = \mathbf{f}(\mathbf{x}, \omega) \quad \forall\ \mathbf{x} \in \mathcal{D}, \tag{27a}$$

$$\gamma_{\mathrm{N}} \mathbf{u}(\mathbf{x}, \omega) + \frac{1}{2} \mathsf{D}^{-1}(\mathbf{x}) \gamma_{\mathrm{D}} \mathbf{u}(\mathbf{x}, \omega) = \mathbf{0}, \qquad \forall\ \mathbf{x} \in \partial\mathcal{D}, \tag{27b}$$

where $\mathbf{u}$ now lies in the Bochner space $L^1(\Omega, \mathbb{P}, X)$ and $\mathbf{f}$ in $L^1(\Omega, \mathbb{P}, Z)$ with the deterministic linear operator $\mathbb{D}$ defined in (10). As in section 4.1, we can take the expectation on both sides of (27a) and (27b), and since spaces $H^1(\mathcal{D})$, $H^r(\partial\mathcal{D})$, for $|r| \leq \frac{1}{2}$, are separable, and operators $\mathbb{D}$, γ_{N}, and γ_{D} linear and deterministic, property (18) holds. Consequently, the strong first moment problem can be stated as follows.

Problem 4.2. Let $\mathbf{f} \in L^1(\Omega, \mathbb{P}, Z)$ with $\bar{\mathbf{f}} = \mathbb{E}[\mathbf{f}] \in Z$. We seek $\bar{\mathbf{u}} = \mathbb{E}[\mathbf{u}] \in X$ such that

$$\mathbb{D}\, \bar{\mathbf{u}} = \bar{\mathbf{f}} \quad \text{in } Z, \tag{28a}$$

$$\gamma_{\mathrm{N}} \bar{\mathbf{u}} + \frac{1}{2} \mathsf{D}^{-1} \gamma_{\mathrm{D}} \bar{\mathbf{u}} = \mathbf{0} \quad \text{on } \left[H^{-\frac{1}{2}}(\partial\mathcal{D}) \right]^{N_E}. \tag{28b}$$

4.2.2. Variational formulation. By Corollary 3.4 and recalling the definition of the bilinear form $\mathsf{d}(\cdot, \cdot)$ in (13), one can quickly derive the next result.

PROPOSITION 4.3. *Let* $\mathbf{f} \in L^1(\Omega, \mathbb{P}, Z)$ *with mean* $\bar{\mathbf{f}} \in Z$*. Then, the first order moment variational problem—seek* $\bar{\mathbf{u}} \in X$ *such that*

$$\mathsf{d}(\bar{\mathbf{u}}, \mathbf{v}) = \sum_{e=1}^{N_E} \left\langle \bar{f}^{(e)}, v^{(e)} \right\rangle_{\mathcal{D}} \tag{29}$$

for all $\mathbf{v} \in X$ *with* $\mathbf{v} = \left(v^{(1)}, \ldots, v^{(N_E)} \right)$*—has a unique solution continuously dependent on the data.*

4.3. Second statistical moment problem. We are interested in computing not only the first order but the second order moment as well so as to have more statistical information related to the neutron flux. Observe that this implies knowledge of the source's statistical second order moments $\mathcal{M}^2\mathbf{f}$. The following derivation is reminiscent of the one performed by Harbrecht [14].

4.3.1. Strong formulation. Let $\mathbf{f} \in L^2(\Omega, \mathbb{P}, Z)$. Then, $\mathbf{u} \in L^2(\Omega, \mathbb{P}, X)$ and we may take expectations of the tensor product of (27a) with itself. This yields

$$\mathcal{M}^2[\mathbb{D}\,\mathbf{u}] = \mathcal{M}^2\mathbf{f} \ \text{ in } Z^{(2)} \tag{30}$$

as $\mathbb{D} \in \mathcal{L}(X, Z)$ and where $Z^{(2)} = Z \otimes Z$. When tensorizing, particular attention should be given to the tensor product space structures encoded in the definitions of spaces X, Z. Specifically,

$$X^{(2)} = X \otimes X = [H^1(\mathcal{D})]^{N_E} \otimes [H^1(\mathcal{D})]^{N_E} = [H^1(\mathcal{D}) \otimes H^1(\mathcal{D})]^{N_E \times N_E}.$$

For $r > 0$, let us define the bivariate spaces $H^r_{mix}(\mathcal{D} \times \mathcal{D}) := H^r(\mathcal{D}) \otimes H^r(\mathcal{D})$ and similarly for dual spaces. Then, for $s \geq 0$, we can identify

$$(X^s)^{(2)} = [H^{1+s}_{mix}(\mathcal{D} \times \mathcal{D})]^{N_E \times N_E} \text{ and } (Z^s)^{(2)} = [\widetilde{H}^{-1+s}_{mix}(\mathcal{D} \times \mathcal{D})]^{N_E \times N_E}. \tag{31}$$

To further simplify notation, we define

$$U(\mathbf{x}, \mathbf{y}) := (\mathcal{M}^2\mathbf{u})(\mathbf{x}, \mathbf{y}) = \mathbb{E}[\mathbf{u} \otimes \mathbf{u}](\mathbf{x}, \mathbf{y}) \in X^{(2)}, \tag{32}$$

$$F(\mathbf{x}, \mathbf{y}) := (\mathcal{M}^2\mathbf{f})(\mathbf{x}, \mathbf{y}) = \mathbb{E}[\mathbf{f} \otimes \mathbf{f}](\mathbf{x}, \mathbf{y}) \in Z^{(2)}. \tag{33}$$

Hence, we can use Proposition 4.1 to write

$$(\mathbb{D} \otimes \mathbb{D})U = F \ \text{ in } Z^{(2)}. \tag{34}$$

For the boundary conditions, the following tensor equation on $\partial\mathcal{D} \times \partial\mathcal{D}$ holds:

$$\begin{aligned} \mathcal{M}^2\left(\gamma_{\mathrm{N}}\mathbf{u}\right) &= \mathcal{M}^2\left(-\frac{1}{2}\mathsf{D}^{-1}\gamma_{\mathrm{D}}\mathbf{u}\right), \\ \left(\gamma_{\mathrm{N}} \otimes \gamma_{\mathrm{N}}\right)U &= \frac{1}{4}\left(\mathsf{D}^{-1}\gamma_{\mathrm{D}} \otimes \mathsf{D}^{-1}\gamma_{\mathrm{D}}\right)U. \end{aligned} \tag{35}$$

These equations are meaningful at least in $H^{-\frac{1}{2}}_{mix}(\partial\mathcal{D}\times\partial\mathcal{D})$ and with more regularity as an equation in $L^2(\partial\mathcal{D} \times \partial\mathcal{D})$. In this last case, we have removed the *mix* subscript as one has $L^2(\partial D \times \partial D) \simeq L^2(\partial D) \otimes L^2(\partial D)$ with $\simeq$ denoting isometric isomorphism of separable Hilbert spaces. Due to the tensorization, we also obtain equations on $\partial\mathcal{D}\times\mathcal{D}$ and $\mathcal{D} \times \partial\mathcal{D}$, as can be seen in the strong form of the second moment problem.

Problem 4.4. For $F \in Z^{(2)}$, seek $U \in X^{(2)}$ such that

$$(\mathbb{D} \otimes \mathbb{D})U = F \qquad \text{in } \mathcal{D} \times \mathcal{D}, \tag{36a}$$

$$(\mathbb{D} \otimes \gamma_{\mathrm{N}})\,U = -\tfrac{1}{2}\left(\mathbb{D} \otimes \mathsf{D}^{-1}\gamma_{\mathrm{D}}\right)U \qquad \text{in } \mathcal{D} \times \partial\mathcal{D}, \tag{36b}$$

$$(\gamma_{\mathrm{N}} \otimes \mathbb{D})\,U = -\tfrac{1}{2}\left(\mathsf{D}^{-1}\gamma_{\mathrm{D}} \otimes \mathbb{D}\right)U \qquad \text{in } \partial\mathcal{D} \times \mathcal{D}, \tag{36c}$$

$$(\gamma_{\mathrm{N}} \otimes \gamma_{\mathrm{N}})\,U = \tfrac{1}{4}\left(\mathsf{D}^{-1}\gamma_{\mathrm{D}} \otimes \mathsf{D}^{-1}\gamma_{\mathrm{D}}\right)U \qquad \text{on } \partial\mathcal{D} \times \partial\mathcal{D}. \tag{36d}$$

Observe that (36b) and (36c) complete the system. Finally, Dirichlet and Neumann trace operators in Problem 4.4 should be interpreted as Cartesian arrays of trace operators per energy group.

4.3.2. Variational formulation. The variational formulation of Problem 4.4 is built by taking duality products of (36a) over $X^{(2)}$. In what follows, we make precise variable dependencies and recall that $X^{(2)} = [H^1_{mix}(\mathcal{D}\times\mathcal{D})]^{N_E\times N_E}$. By integration-by-parts and using (36d), (36b) and (36c), we arrive at the next problem.

Problem 4.5. Seek $U \in X^{(2)}$ such that, for any $F \in Z^{(2)}$, it holds that

$$\mathsf{d}_2(U,V) = \langle F, V\rangle_{\mathcal{D}} \quad \forall\, V \in X^{(2)}, \tag{37}$$

wherein now there is a sum of N_E^2 duality pairings in $H^1_{mix}(\mathcal{D}\times\mathcal{D})$ and the bilinear form $\mathsf{d}_2(\cdot,\cdot)$ is defined as

$$\begin{aligned}\mathsf{d}_2(U,V) := &\sum_{e_1,e_2=1}^{N_E} \mathsf{a}_2^{(e_1e_2)}(U^{(e_1e_2)},V) + \sum_{e_1,\hat e_1,e_2,\hat e_2=1}^{N_E} \mathsf{a}_2^{(\hat e_1\hat e_2 e_1 e_2)}(U^{(\hat e_1\hat e_2)},V)\\ &+ \sum_{e_1,e_2,\hat e_2=1}^{N_E} \mathsf{ab}^{(e_1\hat e_2 e_2)}(U^{(e_1\hat e_2)},V) + \sum_{\hat e_1,e_1,e_2=1}^{N_E} \mathsf{ba}^{(e_1\hat e_1 e_2)}(U^{(\hat e_1 e_2)},V)\end{aligned} \tag{38}$$

for all $V \in H^1_{mix}(\mathcal{D}\times\mathcal{D})$, with the following terms:

$$\begin{aligned}&\mathsf{a}_2^{(e_1e_2)}(U^{(e_1e_2)},V)\\ &\quad:= \int_{\mathcal{D}\times\mathcal{D}} (D^{(e_1)}(\mathbf{x})\nabla_{\mathbf{x}} \otimes D^{(e_2)}(\mathbf{y})\nabla_{\mathbf{y}})U^{(e_1e_2)}(\mathbf{x},\mathbf{y})(\nabla_{\mathbf{x}}\otimes\nabla_{\mathbf{y}})V(\mathbf{x},\mathbf{y})d\mathbf{x}d\mathbf{y}\\ &\qquad+\frac{1}{2}\int_{\mathcal{D}\times\partial\mathcal{D}} (D^{(e_1)}(\mathbf{x})\nabla_{\mathbf{x}}\otimes\gamma_{\mathrm{D}})U^{(e_1e_2)}(\mathbf{x},\mathbf{y})(\nabla_{\mathbf{x}}\otimes\gamma_{\mathrm{D}})V(\mathbf{x},\mathbf{y})d\mathbf{x}ds_{\mathbf{y}}\\ &\qquad+\frac{1}{2}\int_{\partial\mathcal{D}\times\mathcal{D}} (\gamma_{\mathrm{D}}\otimes D^{(e_2)}(\mathbf{y})\nabla_{\mathbf{y}})U^{(e_1e_2)}(\mathbf{x},\mathbf{y})(\gamma_{\mathrm{D}}\otimes\nabla_{\mathbf{y}})V(\mathbf{x},\mathbf{y})ds_{\mathbf{x}}d\mathbf{y}\\ &\qquad+\frac{1}{4}\int_{\partial\mathcal{D}\times\partial\mathcal{D}} (\gamma_{\mathrm{D}}\otimes\gamma_{\mathrm{D}})U^{(e_1e_2)}(\mathbf{x},\mathbf{y})(\gamma_{\mathrm{D}}\otimes\gamma_{\mathrm{D}})V(\mathbf{x},\mathbf{y})ds_{\mathbf{x}}ds_{\mathbf{y}}\\ &\qquad+\int_{\mathcal{D}\times\mathcal{D}} (D^{(e_1)}(\mathbf{x})\nabla_{\mathbf{x}}\otimes\sigma_r^{(e_2)}(\mathbf{y}))U^{(e_1e_2)}(\mathbf{x},\mathbf{y})(\nabla_{\mathbf{x}}\otimes\mathcal{I}_{\mathbf{y}})V(\mathbf{x},\mathbf{y})d\mathbf{x}d\mathbf{y}\\ &\qquad+\int_{\mathcal{D}\times\mathcal{D}} (\sigma_r^{(e_1)}(\mathbf{x})\otimes D^{(e_1)}(\mathbf{y})\nabla_{\mathbf{y}})U^{(e_1e_2)}(\mathbf{x},\mathbf{y})(\mathcal{I}_x\otimes\nabla_{\mathbf{y}})V(\mathbf{x},\mathbf{y})d\mathbf{x}d\mathbf{y}\\ &\qquad+\frac{1}{2}\int_{\mathcal{D}\times\partial\mathcal{D}} (\sigma_r^{(e_1)}(\mathbf{x})\otimes\gamma_{\mathrm{D}})U^{(e_1e_2)}(\mathbf{x},\mathbf{y})(\mathcal{I}_{\mathbf{x}}\otimes\gamma_{\mathrm{D}})V(\mathbf{x},\mathbf{y})d\mathbf{x}ds_{\mathbf{y}}\\ &\qquad+\frac{1}{2}\int_{\partial\mathcal{D}\times\mathcal{D}} (\gamma_{\mathrm{D}}\otimes\sigma_r^{(e_2)}(\mathbf{y}))U^{(e_1e_2)}(\mathbf{x},\mathbf{y})(\gamma_{\mathrm{D}}\otimes\mathcal{I}_{\mathbf{y}})V(\mathbf{x},\mathbf{y})ds_{\mathbf{x}}d\mathbf{y}\\ &\qquad+\int_{\mathcal{D}\times\mathcal{D}} (\sigma_r^{(e_1)}(\mathbf{x})\otimes\sigma_r^{(e_2)}(\mathbf{y}))U^{(e_1e_2)}(\mathbf{x},\mathbf{y})V(\mathbf{x},\mathbf{y})d\mathbf{x}d\mathbf{y},\end{aligned}$$

$$\begin{aligned}&\mathsf{b}_2^{(\hat e_1\hat e_2 e_1 e_2)}(U^{(\hat e_1\hat e_2)},V)\\ &\quad:= -\int_{\mathcal{D}\times\mathcal{D}} (\sigma_s^{(\hat e_1\to e_1)}(\mathbf{x})\otimes\sigma_s^{(\hat e_2\to e_2)}(\mathbf{y}))U^{(\hat e_1\hat e_2)}(\mathbf{x},\mathbf{y})V(\mathbf{x},\mathbf{y})d\mathbf{x}d\mathbf{y},\end{aligned}$$

$$
\begin{aligned}
&\mathsf{ab}^{(e_1\hat{e_2}e_2)}(U^{(e_1\hat{e}_2)}, V) \\
&\quad := \int_{\mathcal{D}\times\mathcal{D}} (D^{(e_1)}(\mathbf{x})\nabla_{\mathbf{x}} \otimes \sigma_s^{(\hat{e}_2\to e_2)}(\mathbf{y}))U^{(e_1\hat{e}_2)}(\mathbf{x},\mathbf{y})(\nabla_{\mathbf{x}} \otimes \mathcal{I}_{\mathbf{y}})V(\mathbf{x},\mathbf{y})d\mathbf{x}d\mathbf{y} \\
&\qquad - \frac{1}{2}\int_{\partial\mathcal{D}\times\mathcal{D}} (\gamma_{\mathrm{D}} \otimes \sigma_s^{(\hat{e}_2\to e_2)}(\mathbf{y}))U^{(e_1\hat{e}_2)}(\mathbf{x},\mathbf{y})V(\mathbf{x},\mathbf{y})d\mathbf{x}d\mathbf{y} \\
&\qquad - \int_{\mathcal{D}\times\mathcal{D}} (\sigma_a^{(e_1)}(\mathbf{x}) \otimes \sigma_s^{(\hat{e}_2\to e_2)}(\mathbf{y}))U^{(e_1\hat{e}_2)}(\mathbf{x},\mathbf{y})V(\mathbf{x},\mathbf{y})d\mathbf{x}d\mathbf{y}.
\end{aligned}
$$

The bilinear form $\mathsf{ba}(\cdot,\cdot)$ follows the same pattern as $\mathsf{ab}(\cdot,\cdot)$ and we skip it for the sake of brevity.

By Corollary 3.4, $\mathbb{D}$ is boundedly invertible, and consequently, direct use of Proposition 4.1 leads to the well-posedness of the tensor deterministic Problem 4.5 for the second order moment.

Proposition 4.6. *Let $\mathbf{f} \in L^2(\Omega, \mathbb{P}, Z)$ with second order moment $F \in Z^{(2)}$. Then, the second order moment variational problem, Problem* 4.5*, has a unique solution $U \in X^{(2)}$ continuously dependent on the data.*

5. Discretization.

We now present the details of the FEM implementation for the multigroup diffusion problem performed as well as associated convergence rates. As stated initially, the main advantage of the deterministic approach for statistical moments relies on the availability of a standard FEM code to solve the tensorized second order moment. We will show that this process never requires actual tensorization and can be efficiently computed with polylogarithmic effort in terms of degrees of freedom. We start by recalling standard results and their application to deterministic estimation of the first order moment, to then compute the second order one.

5.1. Deterministic problem approximation.

We seek to approximate the variational formulation for the nuclear flux diffusion problem (cf. Problem 3.3). We consider a sequence of nested meshes $\{\mathcal{T}_h\}_{N_{elem}(h)\in\mathbb{N}}$, each one composed of triangular elements $\{\tau_t\}_{t=1}^{N_{elem}(h)}$, characterized by a maximum meshwidth $h > 0$ leading to a number of elements $N_{elem}(h)$, and such that

$$
\overline{\mathcal{D}} = \overline{\mathcal{T}}_h = \bigcup_{t=1}^{N_{elem}(h)} \overline{\tau}_t.
$$

Discrete solutions $\mathbf{u}_h$ will belong to the finite element space $[V_h]^{N_E}$, where V_h is defined as

$$
V_h := \{v_h \in H^1(\mathcal{D}) : v_h|_{\tau_t} \in \mathbb{P}_1(\tau_t) \ \ \forall\ t = 1,\dots,N_h\}, \tag{39}
$$

where $N_h = \mathcal{O}(h^2)$ is the total number of degrees of freedom. We will later on refer to mesh discretization levels $L \in \mathbb{N}_0$ with meshwidth h_L and N_L for brevity. Let φ_i^h denote the basis functions of V_h, i.e., $V_h = \operatorname{span}\{\varphi_1^h,\dots,\varphi_{N_h}^h\}$. Then, the Cartesian product approximation space can be written as

$$
[V_h]^{N_E} = \operatorname{span}\{\boldsymbol{\varphi}_i^{h,e}\}_{i,e=1}^{N_h,N_E}
$$

with basis functions $\boldsymbol{\varphi}_i^{h,e}$ defined as

$$
\boldsymbol{\varphi}_i^{h,e}(\mathbf{x}) := \varphi_i^h(\mathbf{x})\hat{c}_e
$$

and $\hat{c}_e \in \mathbb{R}^{N_E}$ is the canonic vector nonzero at group e. Consequently, the unknown

$$\mathbf{u}_h(\mathbf{x}) = \sum_{e=1}^{N_E} \sum_{i=1}^{N_h} \mathrm{u}_i^{(e)} \boldsymbol{\varphi}_i^{h,e}(\mathbf{x}) \tag{40}$$

with $\mathrm{u}_i^{(e)} \in \mathbb{R}$ unknown coefficients. Using (14) and test functions given by the same basis functions $\boldsymbol{\varphi}_i^{h,e}$, we write the discrete version of Problem 3.3.

Problem 5.1. Let $\mathbf{f} \in Z$. Find $\mathbf{u}_h \in [V_h]^{N_E}$ such that

$$\mathsf{d}(\mathbf{u}_h, \mathbf{v}_h) = \langle \mathbf{f}, \mathbf{v}_h \rangle_{\mathcal{D}} \quad \forall\ \mathbf{v}_h \in [V_h]^{N_E} \tag{41}$$

with $\mathsf{d}(\cdot,\cdot)$ as defined in (13).

By conformity and density of the V_h in X and injectivity of $\mathbb{D}$ (cf. Corollary 3.4), one can prove the following result.

LEMMA 5.2 (Theorem 8.11 in [37]). *There exists a refinement level $h_0 > 0$ such that the stability condition*

$$c_s \left\| \mathbf{w}_h \right\|_X \leq \sup_{0 \neq \mathbf{v}_h \in [V_h]^{N_E}} \frac{\mathsf{d}(\mathbf{w}_h, \mathbf{v}_h)}{\left\| \mathbf{v}_h \right\|_X} \quad \forall\ \mathbf{w}_h \in [V_h]^{N_E} \tag{42}$$

holds for all $0 \leq h < h_0$ with a bounded constant $c_s > 0$.

Armed with the above stability condition, we derive the next proposition as in [37, Thm. 8.10].

PROPOSITION 5.3. *Problem* 5.1 *has a unique solution $\mathbf{u}_h \in [V_h]^{N_E}$. Moreover, the best approximation error bound holds*

$$\left\| \mathbf{u} - \mathbf{u}_h \right\|_X \leq \frac{c_{\mathbb{D}}}{c_s} \inf_{0 \neq \mathbf{v}_h \in [V_h]^{N_E}} \left\| \mathbf{u} - \mathbf{v}_h \right\|_X, \tag{43}$$

where $c_{\mathbb{D}}$ is the continuity constant of $\mathbb{D}$.

5.1.1. Matrix formulation. By replacing the discrete solution for the energy group e in the definitions for $\mathsf{a}^{(e)}$ and $\mathsf{b}^{(\hat{e}e)}$ in section 3.2, we derive Galerkin matrices:

$$A^{(e)} := \left(a_{ij}^{(e)} \right)_{i,j=1}^{N_h, N_h}, \quad B^{(e\hat{e})} := \left(b_{ij}^{(e\hat{e})} \right)_{i,j=1}^{N_h, N_h}, \quad \text{and} \quad \mathbf{f}^{(e)} := \left(f_i^{(e)} \right)_{i=1}^{N_h},$$

with

$$a_{ij}^{(e)} := \mathsf{a}^{(e)}(\varphi_j^h, \varphi_i^h), \quad b_{ij}^{(e\hat{e})} := \mathsf{b}^{(e\hat{e})}(\varphi_j^h, \varphi_i^h), \quad f_i^{(e)} := \left\langle f^{(e)}, \varphi_i^h \right\rangle_{\mathcal{D}}, \tag{44}$$

for $e = 1, \ldots, N_E$. Thus, (41) can be equivalently written as the linear system

$$\begin{bmatrix} A^{(1)} & B^{(12)} & \cdots & B^{(1N_E)} \\ B^{(21)} & A^{(2)} & \cdots & B^{(2N_E)} \\ \vdots & \vdots & \ddots & \vdots \\ B^{(N_E 1)} & B^{(N_E 2)} & \cdots & A^{(N_E)} \end{bmatrix} \begin{bmatrix} \mathbf{u}^{(1)} \\ \mathbf{u}^{(2)} \\ \vdots \\ \mathbf{u}^{(N_E)} \end{bmatrix} = \begin{bmatrix} \mathbf{f}^{(1)} \\ \mathbf{f}^{(2)} \\ \vdots \\ \mathbf{f}^{(N_E)} \end{bmatrix}. \tag{45}$$

5.1.2. Discretization error analysis. We now provide theoretical convergence rates for first moment Galerkin problem, Problem 5.1, using piecewise-linear approximation basis. For this, we recall the following standard result.

Lemma 5.4 (Theorem 9.10 in [37]). *Let O be a bounded Lipschitz domain and $u \in H^s(O)$ with $s \in [\beta, 2]$ and $\beta \in \{0,1\}$. Then, there holds the approximation property*

$$\inf_{v_h \in V_h(O)} \|u - v_h\|_{H^\beta(O)} \leq ch^{s-\beta}|u|_{H^s(O)}, \tag{46}$$

where $c > 0$ independent of h, $|\cdot|_{H^s(O)}$ denotes the $H^s(O)$-seminorm, and $V_h(O)$ denotes the space of piecewise linear functions over a mesh on O.

We can derive a general error bound in the Cartesian product space framework by assuming Assumption 3.5 and combining the above lemma with Proposition 5.3.

Proposition 5.5. *Let $\beta = 0, 1$ and $\mathbf{u} \in X^\beta$ and $\mathbf{u}_h \in V_h$ denote the continuous and discrete solutions of Problems* 3.3 *and* 5.1*, respectively. Then, the following error bound holds:*

$$\|\mathbf{u} - \mathbf{u}_h\|_{X^\beta} \leq ch^{s-\beta} \sum_{e=1}^{N_E} \left|u^{(e)}\right|_{H^s(\mathcal{D})} \tag{47}$$

for $s \in [\beta, 2]$ and with a constant $c > 0$.

Alternatively, we can obtain a better description of the constant above by using Cea's lemma [37, Thm. 8.1] and Theorem 5.4. Specifically, we can derive the following error bound for the first energy group.

Proposition 5.6. *Assume there is only down-scattering and $u^{(1)} \in H^\beta(\mathcal{D})$, with $\beta \in \{0,1\}$. Then, it holds that*

$$\left\|u^{(1)} - u_h^{(1)}\right\|_{H^\beta(\mathcal{D})} \leq c\frac{c_2^{\mathcal{A}^{(1)}}}{c_1^{\mathcal{A}^{(1)}}} h^{s-\beta} \left|u^{(1)}\right|_{H^s(\mathcal{D})} \tag{48}$$

with $s \in [\beta, 2]$, constants $c_2^{\mathcal{A}^{(1)}}$ and $c_1^{\mathcal{A}^{(1)}}$ being continuity and coercivity constants of the operator $\mathcal{A}^{(1)}$, and $c > 0$ independent of h.

In general, the same inequality for all the energy groups does not hold due to the lack of Galerkin orthogonality. Consequently, the interaction between the energy groups generates a dependence between the errors of different groups. Theorem 5.7 states the relation between every group with the first one in a down-scattering diffusion multigroup equation.

Theorem 5.7. *For the down-scattering problem, i.e.,* (45)*, with $\mathcal{B}^{(e_1 e_2)} = 0$ for all $e_1 < e_2$, the error of approximate solution for an specific energy group e is bounded as*

$$\begin{aligned}\left\|u^{(e)} - u_h^{(e)}\right\|_\beta \leq{}& ch^{s-\beta} \frac{c_2^{\mathcal{A}^{(e)}}}{c_1^{\mathcal{A}^{(e)}}} \left|u^{(e)}\right|_s + ch^{s-\beta} \sum_{\hat{e}=1}^{e-2} K^{(e\hat{e})} \left|u^{(\hat{e})}\right|_s \\ &+ ch^{s-\beta} \sum_{e'=1}^{e-1} 2^{e-e'} \left(\prod_{\hat{e}=e'}^{e-1} \frac{c^{(\hat{e}+1,\hat{e})}}{c_1^{\mathcal{A}^{(\hat{e}+1)}}}\right) \frac{c_2^{\mathcal{A}^{(e')}}}{c_1^{\mathcal{A}^{e'}}} \left|u^{(e')}\right|_s,\end{aligned} \tag{49}$$

where $c > 0$ independent of h.

Proof. See Appendix A. ∎

Remark 5.8. This last result implies that the error of the first level is systematically propagated to all the other levels. The same happens with each level lower than e. As we can see, the higher the σ_s values are and the lower the ellipticity constant is, the worse the error bound obtained. Moreover, this will occur in any forward energy level finite element solving scheme irrespective of whether deterministic or uncertain conditions are employed. Surprisingly, this condition has, to our knowledge, not yet been reported in the literature.

5.2. Approximations of first and second moments. For the first moment problem described in section 4.2.2, we simply require solving Problem 5.1 with a right-hand side equal to the expectation of the source $\bar{\mathbf{f}}$ using the standard FEM. The Galerkin matrices obtained will be reused for the second moment computation as follows.

For the second statistical moment (cf. Problem 4.5), we recall that each element $U^{(e_1 e_2)}$ in the Hilbertian tensor product space $H^1_{mix}(\mathcal{D}\times\mathcal{D})$, with $e_1, e_2 \in \{1, \ldots, N_E\}$, can be approximated as a limit, in this norm, of tensor product elements

$$U^{(e_1 e_2)} = u^{(e_1)} \otimes u^{(e_2)},$$

with $u^{(e_1)}$ and $u^{(e_2)}$ in $H^1(\mathcal{D})$ built using the associate infinite dimensional orthornormal basis. These in turn can be approximated via finite linear combinations of $u_h^{(e_1)} \in V_h$ and $u_{\tilde{h}}^{(e_2)} \in V_{\tilde{h}}$, conforming finite element spaces in $H^1(\mathcal{D})$ as defined in (39), with meshwidths h and $\tilde{h}$ not necessarily equal, i.e., N_h and $N_{\tilde{h}}$ may differ. In other words, we will seek

$$U_{h,\tilde{h}}^{(e_1 e_2)} \in V_{h,\tilde{h}} := V_h \otimes V_{\tilde{h}},$$

where $N_{h,\tilde{h}} := \dim(V_{h,\tilde{h}}) = N_h \cdot N_{\tilde{h}}$.

We can now state the discrete version of Problem 4.5.

Problem 5.9. Seek $U_h \in [V_{h,\tilde{h}}]^{N_E \times N_E}$ such that, for any $F \in Z^{(2)}$, it holds that

$$\mathsf{d}_2(U_{h\tilde{h}}, W_{h\tilde{h}}) = \left\langle F, W_{h\tilde{h}} \right\rangle_{\mathcal{D}} \quad \forall\, W_h \in [V_{h,\tilde{h}}]^{N_E \times N_E}, \tag{50}$$

where the bilinear form $\mathsf{d}_2(\cdot,\cdot)$ is defined as in (38).

5.2.1. Matrix formulation. As before, one can define finite dimensional Cartesian product spaces,

$$[V_h]^{N_E} = \mathrm{span}\{\boldsymbol{\varphi}_i^{h,e}\}_{i,e=1}^{N_h,N_E}, \quad [V_{\tilde{h}}]^{N_E} = \mathrm{span}\{\boldsymbol{\varphi}_i^{\tilde{h},e}\}_{i,e=1}^{N_{\tilde{h}},N_E}, \tag{51}$$

with $\boldsymbol{\varphi}_i^{h,e}$ and $\boldsymbol{\varphi}_i^{\tilde{h},e}$ as in section 5.1. Then,

$$\mathbf{u}_h(\mathbf{x}) = \sum_{e_1=1}^{N_E} \sum_{i=1}^{N_h} \mathrm{d}_i^{(e_1)} \boldsymbol{\varphi}_i^{h,e_1}(\mathbf{x}) = \sum_{i=1}^{N_h} \mathbf{d}_i \varphi_i^h(\mathbf{x}), \tag{52}$$

$$\mathbf{u}_{\tilde{h}}(\mathbf{y}) = \sum_{e_2=1}^{N_E} \sum_{j=1}^{N_{\tilde{h}}} \tilde{\mathrm{d}}_j^{(e_2)} \boldsymbol{\varphi}_j^{\tilde{h},e_2}(\mathbf{y}) = \sum_{j=1}^{N_{\tilde{h}}} \tilde{\mathbf{d}}_j \varphi_j^{\tilde{h}}(\mathbf{y}). \tag{53}$$

With these, we can write

$$
\begin{aligned}
U_{h,\tilde{h}}(\mathbf{x},\mathbf{y}) &= \left(\sum_{e_1=1}^{N_E}\sum_{i=1}^{N_h} \mathrm{d}_i^{(e_1)}\boldsymbol{\varphi}_i^{h,e_1}(\mathbf{x})\right)\left(\sum_{e_2=1}^{N_E}\sum_{j=1}^{N_{\tilde{h}}} \tilde{\mathrm{d}}_j^{(e_2)}\boldsymbol{\varphi}_j^{\tilde{h},e_2}(\mathbf{y})\right)^{\top} \\
&= \sum_{i=1}^{N_h}\sum_{j=1}^{N_{\tilde{h}}} \mathbf{d}_i\tilde{\mathbf{d}}_j^{\top}(\varphi_i^h\otimes\varphi_j^{\tilde{h}})(\mathbf{x},\mathbf{y}),
\end{aligned} \tag{54}
$$

where $\mathbf{d}_i, \tilde{\mathbf{d}}_j \in \mathbb{R}^{N_E}$ are unknown coefficient vectors for $i = 1,\dots,N_h$ and $j = 1,\dots,N_{\tilde{h}}$, respectively. Replacing (54) in (50) and using as test functions the tensor basis

$$
\left\{\boldsymbol{\varphi}_i^{h,e_1}(\mathbf{x})\boldsymbol{\varphi}_j^{\tilde{h},e_2}(\mathbf{y})^{\top}\right\}_{i,j,e_1,e_2=1}^{N_h,N_{\tilde{h}},N_E,N_E},
$$

we obtain the following linear system:

$$
\left(\sum_{k=1}^{N_h} A_{ik}\mathbf{d}_k\right)\left(\sum_{l=1}^{N_{\tilde{h}}} \widetilde{A}_{jl}\tilde{\mathbf{d}}_l\right)^{\top} = \mathbf{Q}_{ij}\ \forall\ i=1,\dots,N_h,\ \forall\ j=1,\dots,N_{\tilde{h}}, \tag{55}
$$

where the matrices $A_{ik} \in \mathbb{R}^{N_E\times N_E}$, for all $i,k = 1,\dots,N_h$ and $\widetilde{A}_{jl} \in \mathbb{R}^{N_E\times N_E}$ for all $j,l = 1,\dots,N_{\tilde{h}}$, are defined as

$$
A_{ik} := \begin{bmatrix} a_{ik}^{(1)} & b_{ik}^{(12)} & \dots & b_{ik}^{(1N_E)} \\ b_{ik}^{(21)} & a_{ik}^{(2)} & \dots & b_{ik}^{(2N_E)} \\ \vdots & \vdots & \ddots & \vdots \\ b_{ik}^{(N_E1)} & b_{ik}^{(N_E2)} & \dots & a_{ik}^{(N_EN_E)} \end{bmatrix},\ \widetilde{A}_{jl} := \begin{bmatrix} \widetilde{a}_{jl}^{(1)} & \widetilde{b}_{jl}^{(12)} & \dots & \widetilde{b}_{jl}^{(1N_E)} \\ \widetilde{b}_{jl}^{(21)} & \widetilde{a}_{jl}^{(2)} & \dots & \widetilde{b}_{jl}^{(2N_E)} \\ \vdots & \vdots & \ddots & \vdots \\ \widetilde{b}_{jl}^{(N_E1)} & \widetilde{b}_{jl}^{(N_E2)} & \dots & \widetilde{a}_{jl}^{(N_EN_E)} \end{bmatrix},
$$

where entries $a_{ik}^{(e_1)}$, $b_{ik}^{(e_1\hat{e}_1)}$ (resp., $\widetilde{a}_{jl}^{(e_2)}$, $\widetilde{b}_{jl}^{(e_2\hat{e}_2)}$) are defined over V_h (resp., $V_{\tilde{h}}$) as in (44) for $e_1, \hat{e}_1 = 1,\dots,N_E$. The second moment source terms $\mathbf{Q}_{ij} \in \mathbb{R}^{N_E\times N_E}$ are defined as

$$
\mathbf{Q}_{ij} := \int_{\mathcal{D}\times\mathcal{D}} F(\mathbf{x},\mathbf{y})\varphi_i^h(\mathbf{x})\varphi_j^{\tilde{h}}(\mathbf{y})d\mathbf{x}d\mathbf{y}, \tag{56}
$$

for $i = 1,\dots,N_h$ and $j = 1,\dots,N_{\tilde{h}}$. Equivalently, one can write (55) as

$$
\sum_{k=1}^{N_h}\sum_{l=1}^{N_{\tilde{h}}} A_{ik}\mathbf{D}_{kl}\widetilde{A}_{jl}^{\top} = \mathbf{Q}_{ij}, \tag{57}
$$

where $\mathbf{D}_{kl} := \mathbf{d}_k\tilde{\mathbf{d}}_l^{\top} \in \mathbb{R}^{N_E\times N_E}$. This is equivalent to the following matrix system:

$$
\begin{bmatrix}
A_{11}\begin{bmatrix} \widetilde{A}_{11}^{\top} & \dots & \widetilde{A}_{1N_{\hat{h}}}^{\top} \\ \vdots & \ddots & \vdots \\ \widetilde{A}_{N_{\hat{h}}1}^{\top} & \dots & \widetilde{A}_{N_{\hat{h}}N_{\hat{h}}}^{\top} \end{bmatrix} & \dots & A_{1N_h}\begin{bmatrix} \widetilde{A}_{11}^{\top} & \dots & \widetilde{A}_{1N_{\hat{h}}}^{\top} \\ \vdots & \ddots & \vdots \\ \widetilde{A}_{N_{\hat{h}}}^{\top} & \dots & \widetilde{A}_{N_{\hat{h}}N_{\hat{h}}}^{\top} \end{bmatrix} \\
\vdots & \ddots & \\
A_{N_h1}\begin{bmatrix} \widetilde{A}_{11}^{\top} & \dots & \widetilde{A}_{1N_{\hat{h}}}^{\top} \\ \vdots & \ddots & \vdots \\ \widetilde{A}_{N_{\hat{h}}1}^{\top} & \dots & \widetilde{A}_{N_{\hat{h}}N_{\hat{h}}}^{\top} \end{bmatrix} & \dots & A_{N_hN_h}^{\top}\begin{bmatrix} \widetilde{A}_{11}^{\top} & \dots & \widetilde{A}_{1N_{\hat{h}}}^{\top} \\ \vdots & \ddots & \vdots \\ \widetilde{A}_{N_h1}^{\top} & \dots & \widetilde{A}_{N_{\hat{h}}N_{\hat{h}}}^{\top} \end{bmatrix}
\end{bmatrix}
\begin{bmatrix} \mathbf{D}_{11} \\ \vdots \\ \mathbf{D}_{1N_{\hat{h}}} \\ \vdots \\ \mathbf{D}_{N_h1} \\ \vdots \\ \mathbf{D}_{N_hN_{\hat{h}}} \end{bmatrix}
=
\begin{bmatrix} \mathbf{Q}_{11} \\ \vdots \\ \mathbf{Q}_{1N_{\hat{h}}} \\ \vdots \\ \mathbf{Q}_{N_h1} \\ \vdots \\ \mathbf{Q}_{N_hN_{\hat{h}}} \end{bmatrix}. \tag{58}
$$

Clearly, the above linear system has enormously increased the number of unknowns as the curse of dimensionality would predict.

PROPOSITION 5.10. *Define*

$$\mathbf{A} := \begin{bmatrix} A_{11} & \dots & A_{1N_h} \\ \vdots & \ddots & \vdots \\ A_{N_h 1} & \cdots & A_{N_h N_h} \end{bmatrix}, \qquad \widetilde{\mathbf{A}} := \begin{bmatrix} \widetilde{A}_{11} & \dots & \widetilde{A}_{1N_{\hat{h}}} \\ \vdots & \ddots & \vdots \\ \widetilde{A}_{N_{\hat{h}} 1} & \cdots & \widetilde{A}_{N_{\hat{h}} A_{\hat{h}}} \end{bmatrix}. \tag{59}$$

Then, (58) *can be equivalently written as*

$$\mathbf{A}\mathbf{D}\widetilde{\mathbf{A}}^\top = \mathbf{Q}, \tag{60}$$

where $\mathbf{D} := (\mathbf{D}_{ij})_{i,j=1}^{N_h, N_{\hat{h}}}$ *and* $\mathbf{Q} := (\mathbf{Q}_{ij})_{i,j=1}^{N_h, N_{\hat{h}}}$.

Proof. Let us define $\mathbf{Y} := \mathbf{D}\widetilde{\mathbf{A}}^\top$; then

$$Y_{kj} = \sum_{l=1}^{N_{\hat{h}}} \mathbf{D}_{kl} \left(\widetilde{\mathbf{A}}^\top\right)_{lj} = \sum_{l=1}^{N_{\hat{h}}} \mathbf{D}_{kl} \widetilde{\mathbf{A}}_{jl}^\top.$$

On the other hand, $\mathbf{Q} = \mathbf{A}\mathbf{Y}$, and therefore

$$\mathbf{Q}_{ij} = \sum_{k=1}^{N_{h_0}} A_{ik} Y_{kj} = \sum_{k=1}^{N_h} A_{ik} \sum_{l=1}^{N_{\hat{h}}} \mathbf{D}_{kl} \widetilde{A}_{jl}^\top = \sum_{k=1}^{N_h} \sum_{l=1}^{N_{\hat{h}}} A_{ik} \mathbf{D}_{kl} \widetilde{A}_{jl}^\top$$

as stated. ∎

Proposition 5.10 is important because it avoids dealing with the huge matrix system given by (58). Instead, we solve (60) in two steps,

$$\mathbf{A}\mathbf{Y} = \mathbf{Q} \quad \text{and} \quad \widetilde{\mathbf{A}}\mathbf{D}^\top = \mathbf{Y}^\top. \tag{61}$$

One may wonder whether one could exploit for computational purposes choices h and $\hat{h}$. Indeed, one can compute the second moment using $\hat{h} = h$ and carry out a *full tensor discretization*. However, a *sparse* approximation will be shown to exist with considerable gains.

5.2.2. Full tensor approximation. We now switch notation from h to L, to explicitly declare the dependence of solutions on mesh refinement levels $L \in \mathbb{N}_0$ with associated spaces $V_L \equiv V_{h_L}$. Thus, we will seek solutions U_L in the tensor space:

$$V_{L,L}^{N_E} := [V_L \otimes V_L]^{N_E \times N_E}$$

with $N_{L,L} := \dim(V_{L,L}) = N_L^2$. Following directly from Lemma 5.2, we can derive the next stability result.

LEMMA 5.11. *There exists* $L_0 \in \mathbb{N}$ *and* $c_S > 0$ *such that for all* $L \geq L_0$,

$$\inf_{0 \neq U \in V_{L,L}^{N_E}} \sup_{0 \neq W \in V_{L,L}^{N_E}} \frac{\mathsf{d}_2(U, W)}{\|U\|_{X^{(2)}} \|W\|_{X^{(2)}}} \geq \frac{1}{c_S} > 0, \tag{62}$$

and where $c_S = c_s^2$ *with* c_s *being the mean-field inf-sup constant introduced in Lemma* 5.2.

With this tensor inf-sup condition, one can easily show that the full tensor product approximation for Problem 5.9 is unique.

PROPOSITION 5.12. *Problem* 5.9 *has a unique discrete solution* $U_{L,L} \in V_{L,L}^{N_E}$. *Moreover, if* $U \in X^{(2)}$ *denotes the solution of the continuous Problem* 4.5, *then*

$$\|U - U_{L,L}\|_{X^{(2)}} \leq c \inf_{W_{L,L} \in V_{L,L}^{N_E}} \|U - W_h\|_{X^{(2)}} \tag{63}$$

with $c > 0$ *bounded independently of* L.

Since basis elements are chosen equal in each variable, $\mathbf{A} = \widetilde{\mathbf{A}}$. Consequently, we just need to solve (61) computing only one matrix. However, the total number of degrees of freedom using this full tensor technique is equal to $(N_L \cdot N_E)^2$, showing a quadratic increases in L, which calls for large computational efforts.

5.2.3. Sparse tensor approximation. To tackle the curse of dimensionality, we introduce the sparse tensor approach following [40] and later references [16, 19]. In a nutshell, the idea is to reduce the number of degrees of freedom by solving over a subspace of $V_{L,L}$.

For a nested sequence of meshes and associated finite element spaces $\{V_l\}_{l=0}^{L}$, one can define detail spaces W_l as

$$W_l := (P_l - P_{l-1})H^1(\mathcal{D}) \subset V_l, \quad l \geq 1,$$

where P_l is the projection into V_l space. Hence, one can write $V_L = W_L \oplus V_{L-1}$ and deduce

$$V_L = \bigoplus_{l=0}^{L} W_l,$$

where $W_0 := V_0$. The sparse tensor approximation consists of looking for the solution in the tensor space

$$\widehat{V}_{L,L_0} = \bigoplus_{\substack{2L_0 \leq l_1 + l_2 \leq L + L_0 \\ L_0 \leq l_1, l_2 \leq L}} (W_{l_1} \otimes W_{l_2}), \tag{64}$$

where $L_0 \geq 0$ shall be referred to as the *minimal resolution level.* This value is related to the threshold mesh required for asymptotic convergence and is characteristic of indefinite or coercive problems [19, 21].

Similar to the full tensor case, let us define

$$\widehat{V}_{L,L_0}^{N_E} := [\widehat{V}_{L,L_0}]^{N_E \times N_E}.$$

Then, we can state the next stability condition.

LEMMA 5.13 (Theorem 5.2 in [40]). *There exists* $L_0 \in \mathbb{N}$ *and* $\hat{c}_S > 0$ *such that for all* $L \geq L_0$,

$$\inf_{0 \neq \widehat{U} \in \widehat{V}_{L,L_0}^{N_E}} \sup_{0 \neq \widehat{W} \in \widehat{V}_{L,L_0}^{N_E}} \frac{\mathsf{d}_2(\widehat{U}, \widehat{W})}{\left\|\widehat{U}\right\|_{X^{(2)}} \left\|\widehat{W}\right\|_{X^{(2)}}} \geq \frac{1}{\hat{c}_S} > 0. \tag{65}$$

Moreover, the discrete problem is well posed.

PROPOSITION 5.14. *Let* $L_0 \in \mathbb{N}$ *and* $U \in X^{(2)}$ *be the solution of Problem* 4.5. *Then, for any* $L \geq L_0$ *the sparse tensor version of Problem* 5.1 *has a unique solution* $\widehat{U}_{L,L_0} \in \widehat{V}_{L,L_0}^{N_E}$. *Moreover, it holds that*

$$\left\| U - \widehat{U}_{L,L_0} \right\|_{X^{(2)}} \leq c \inf_{\widehat{W}_{L,L_0} \in \widehat{V}_{L,L_0}^{N_E}} \left\| U - \widehat{W}_{L,L_0} \right\|_{X^{(2)}} \tag{66}$$

with $c > 0$ *bounded independent of* L.

5.2.4. Convergence errors. Convergence rates for the full tensor approximation are obtained in a similar way to those for the first moment problem and we recall Assumption 3.5.

Denote the continuous solution $U^{(e_1 e_2)} \in H^1_{mix}(\mathcal{D} \times \mathcal{D})$ and $U_{L,L}^{(e_1 e_2)} \in V_{L,L}$ its full tensor Galerkin approximation. Then, by Proposition 5.12, it holds that

$$\left\| U^{(e_1 e_2)} - U_{L,L}^{(e_1 e_2)} \right\|_{L^2(\mathcal{D} \times \mathcal{D})} \leq C \inf_{W_{L,L} \in V_{L,L}} \left\| U^{(e_1 e_2)} - W_{L,L} \right\|_{L^2(\mathcal{D} \times \mathcal{D})}. \tag{67}$$

Then, by Theorem 5.4 with $O = \mathcal{D} \times \mathcal{D}$, we have the following result:

$$\left\| U^{(e_1 e_2)} - U_{L,L}^{(e_1 e_2)} \right\|_{H^\sigma(\mathcal{D} \times \mathcal{D})} \leq C h_L^{s-\sigma} \left| U^{(e_1 e_2)} \right|_{H^s(\mathcal{D} \times \mathcal{D})}. \tag{68}$$

More generally, we can write as follows.

PROPOSITION 5.15. *Let* $\beta = 0, 1$. *Denote by* $U \in (X^\beta)^{(2)}$ *and* $U_{L,L} \in V_{L,L}^{N_E}$ *the solutions of Problems* 4.5 *and* 5.9, *respectively. Then, it holds that*

$$\| U - U_{L,L} \|_{(X^\beta)^{(2)}} \leq c h_L^{s-\beta} \sum_{e_1, e_2 = 1}^{N_E} \left| U^{(e_1 e_2)} \right|_{H^s(\mathcal{D} \times \mathcal{D})} \tag{69}$$

for $s \in [\beta, 2]$ *and with a constant* $c > 0$ *independent of* L.

Observe that the convergence rate in terms of h is the same for full tensor and first moment. However, in terms of degrees of freedom it differs, because $h = \mathcal{O}(N_L^{-2})$ and $h = \mathcal{O}(N_{L,L}^{-4})$ for first moment and full tensor approximations, respectively.

To state the theoretical result for the sparse tensor approximation we use Theorem 5.3 in [40].

PROPOSITION 5.16. *Assume* $\mathbf{f} \in L^2(\Omega, \mathbb{P}, Z^s)$ *with expectation* $\bar{\mathbf{f}}$ *and let* $U \in X^{(2)}$ *and* $\widehat{U}_{L,L_0} \in V_{L,L_0}^{N_E}$ *denote the solutions for the continuous and discrete second moment problems, Problems* 4.5 *and* 5.9, *respectively. Then, for* $0 \leq s \leq 1$, *it holds that*

$$\left\| U - \widehat{U}_{L,L_0} \right\|_{X^{(2)}} \leq C N_L^{-\frac{s}{2}} \sqrt{\log N_L} \left\| \bar{\mathbf{f}} \right\|_{Z^s}. \tag{70}$$

5.3. Combination technique. When working with meshes in more than one dimension it is hard to find explicitly basis functions for detail spaces W_l. Hence, we use the so-called combination technique [15] to express (64) as sums of spaces $V_{l_1} \otimes V_{l_2}$. Specifically, one can write

$$\widehat{V}_{L,L_0} = \bigoplus_{l_1 = L_0}^{L} V_{L+L_0-l_1} \otimes V_{l_1} - \bigoplus_{l_2 = L_0}^{L} V_{l_2} \otimes V_{L+L_0-l_2}. \tag{71}$$

Thus, when looking for the solution $\widehat{U}_{L,L_0} \in \widehat{V}_{L,L_0}^{N_E}$, one needs to solve different linear systems over the tensor product spaces in (71). These individual solutions are then adequately superposed following the formula above to yield the desired final approximation.

6. Numerical results and discussion for a homogeneous domain.

6.1. Domain and parameters. The domain $\mathcal{D} \in \mathcal{R}^2$ chosen for this problem is defined as $\mathcal{D} := \{(x_1, x_2) \in \mathbb{R}^2 : 0 \leq x_1 \leq 12, 0 \leq x_2 \leq 12\}$. This domain is made up of water, whose parameters are shown in Table 1 in the column corresponding to domain $\mathcal{D}_b$.

Meshes were constructed using the software GMSH,[1] with refinement done by splitting. As a result of this procedure, we obtained seven nested meshes defining seven different discretization levels (L), with subspaces denoted by V_L, $L = 1, \ldots, 7$. Again, we denote by N_L the number of degrees of freedom for each discretization level. To compute the FEM matrices we used FEniCS in Python.

6.2. Analytic solution. First, we built the problem for a known analytic solution using the method of manufactured solutions [24, 22, 28], in order to analyze the error between this and the discrete approximate solution. We will use a solution with general form given by

$$u^{(e)}(\mathbf{x}) = \frac{1}{D^{(e)}} \left(1 + \alpha^{(e)} x_1 + \beta^{(e)} x_1^2\right) \left(1 + \alpha^{(e)} x_2 + \beta^{(e)} x_2^2\right), \tag{72}$$

where $\alpha^{(e)}$ and $\beta^{(e)}$ are such that $u^{(e)}$ satisfies the boundary conditions given by equation (5). It holds that

$$\alpha^{(e)} = \frac{1}{2D^{(e)}}, \qquad \beta^{(e)} = -\frac{(2 + 12\alpha^{(e)})}{(48D^{(e)} + 12^2)}.$$

6.3. First moment convergence. In Figure 1 we show the error between the discrete and analytic solutions for the first moment, at six different discretization

TABLE 1

Removal cross section (σ_r), diffusion coefficient (D), and source (μ) logarithmic values for each energy group and each subdomain used for the nonhomogeneous problem. Numbers in parentheses give the logarithm of the midpoint energy for each group in MeV. Values for D_b are used for the homogeneous case.

	$\sigma_r^{(e)}$			$D^{(e)}$			
e	$\mathcal{D}_b$	$\mathcal{D}_a$	$\mathcal{D}_s$	$\mathcal{D}_b$	$\mathcal{D}_a$	$\mathcal{D}_s$	μ
1 (1.04)	-1.104	-0.435	-0.641	0.294	0.621	0.266	1.04
2 (0.774)	-1.087	-0.566	-0.621	0.253	0.506	0.23	0.774
3 (0.509)	-0.952	-1.1	-0.595	0.199	0.338	0.241	0.509
4 (0.244)	-0.784	-2.537	-0.63	0.163	0.196	0.172	0.244
5 (-0.021)	-0.642	-2.582	-0.749	0.148	0.005	0.178	-0.021
6 (-0.287)	-0.484	-2.539	-0.953	0.075	-0.102	0.173	-0.287
7 (-0.552)	-0.372	-2.31	-1.031	-0.038	-0.208	-0.084	-0.552
8 (-0.817)	-0.259	-2.226	-1.074	-0.127	-0.296	-0.173	-0.817
9 (-1.082)	-0.167	-2.147	-1.145	-0.195	-0.376	-0.261	-1.082
10 (-1.347)	-0.1	-2.156	-1.356	-0.23	-0.437	-0.253	-1.347
11 (-1.689)	-0.204	-2.592	-1.387	-0.231	-0.395	-0.273	-1.689
12 (-2.22)	-0.169	-2.582	-1.472	-0.222	-0.428	-0.285	-2.22
13 (-2.752)	-0.157	-2.579	-1.525	-0.164	-0.438	-0.288	-2.752
14 (-3.283)	-0.154	-2.578	-1.429	-0.111	-0.442	-0.289	-3.283
15 (-3.814)	-0.153	-2.578	-1.248	-0.171	-0.443	-0.289	-3.814
16 (-4.345)	-0.152	-2.578	-1.103	-0.028	-0.443	-0.289	-4.345
17 (-4.877)	-0.151	-2.577	-1.324	-0.067	-0.444	-0.289	-4.877
18 (-5.408)	-0.15	-2.577	-0.665	-0.367	-0.445	-0.289	-5.408
19 (-6.05)	-2.027	-4.746	1.086	-1.6	-0.442	-0.29	-6.05
20 (-8.676)	0.541	-4.242	1.677	-2.154	-1.344	-0.316	-8.676

[1] Available at http://gmsh.info/.

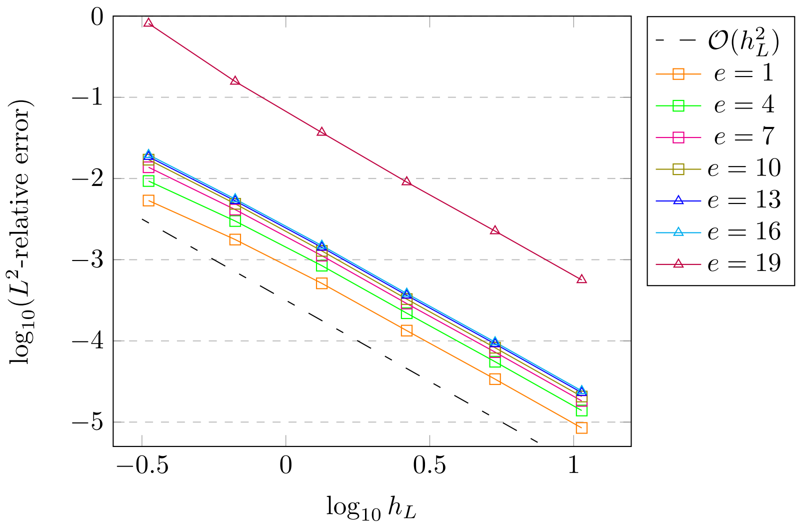

Fig. 1. *Homogeneous problem: L^2-relative error between discrete $u_L^{(e)}$ and analytic $u^{(e)}$ solutions for $L = 1, \dots, 6$. Convergence is $\mathcal{O}(h_L^2)$ as expected from Proposition* 5.5 *with $\beta = 0$. Curves for other energy groups display the same slope but are shifted up as predicted by Theorem* 5.7.

levels. Each curve represents the error convergence of a specific energy group as we refine the mesh with convergence rate $\mathcal{O}(h_L^2)$ as expected from the $s = 2$ regularity of (72) (cf. Theorem 5.4). We also observe that the error is lower for the first energy group and increases with each subsequent group. This confirms the results in section 5.1.2: when in down-scattering, bounds of higher energy groups follow a nondecreasing function of the lower energy groups' error.

6.4. Second moment convergence. For the second moment computation, in Figure 2 we compare the errors from the sparse and full tensor methods with respect to the analytic solution. As we expected, the sparse tensor requires fewer degrees of freedom than the full version to achieve a given error. Furthermore, the rate of H^1-error convergence of the full tensor approximation is $\mathcal{O}(N_{L,L}^{-1/4})$, which is equivalent to $\mathcal{O}(N_L^{-1/2})$ and $\mathcal{O}(h_L)$. Moreover, we see the impact of choosing different values L_0 in reaching asymptotic convergence regimes.

To validate the theoretical convergence rates predicted in Proposition 5.16, we plot in Figure 3 convergence errors for sparse tensor approximations in terms of N_L. Our results show that the sparse tensor error convergence agrees with prediction with regularity equal to one.

7. Numerical results and discussion for a nonhomogeneous domain. We now turn to the more interesting case of problems with nonhomogeneities, wherein material properties will vary in space. Let us consider a generic radiation shielding problem where a neutron source, e.g., a plutonium spontaneous fission source, is immersed in water along with a heavy metal absorber, e.g., lead. The problem layout is illustrated in Figure 4.

7.1. Domain and parameters. To describe the domain we are going to define three different regions or subdomains: a bulk media ($\mathcal{D}_b$), a source region ($\mathcal{D}_s$), and an absorption region ($\mathcal{D}_a$):

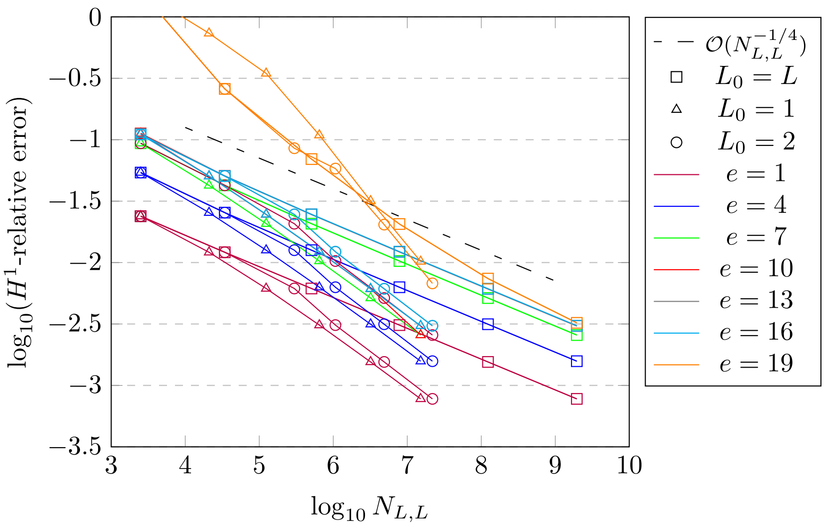

FIG. 2. *Homogeneous problem: H^1-relative error between the discrete $U_{L,L_0}^{(ee)}$ and analytic $U^{(ee)}$ solutions for $e \in \{1,2,3,4\}$, $L = 1,\ldots,6$. Different values for L_0, with $L_0 = L$ corresponding to the full tensor case. For this last one, error convergence rates are $\mathcal{O}(N_{L,L}^{-1/4})$, where $N_{L,L} = N_L^2$ is the total number of degrees of freedom. This convergence is equivalent to $\mathcal{O}(h_L)$, where h_L is the mesh size.*

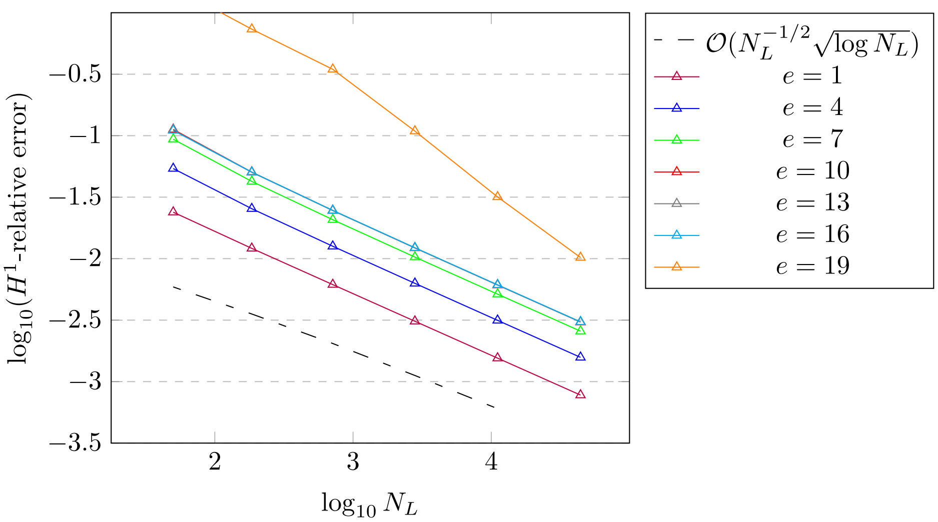

FIG. 3. *Homogeneous problem: H^1-relative error between the discrete solution $\widehat{U}_{L,L_0}^{(ee)}(\mathbf{x},\mathbf{x})$, and the analytic solution $U^{(ee)}(\mathbf{x},\mathbf{x})$ for $L = 1,\ldots,6$ and $L_0 = 1$. The convergence is $\mathcal{O}(N_L^{-1/2}\sqrt{\log N_L})$ as predicted by Proposition* 5.16.

$$\begin{aligned}
\mathcal{D}_s &:= \{(x_1,x_2) \in \mathbb{R}^2 : 2 \le x_1 \le 4,\ 2 \le x_2 \le 4\},\\
\mathcal{D}_a &:= \{(x_2,x_2) \in \mathbb{R}^2 : 0 \le x_1 \le 12,\ 0 \le x_2 \le 12\},\\
\mathcal{D}_b &:= \mathcal{D} \setminus \overline{(\mathcal{D}_s \cup \mathcal{D}_a)}.
\end{aligned}$$

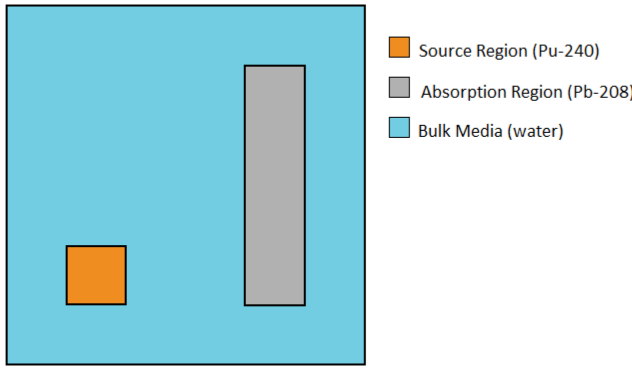

FIG. 4. *Layout of nonhomogeneous problem containing a source, an absorber, and a water background media.*

In the case of a nonhomogeneous domain, $\sigma_a^{(e)}$, $\sigma_s^{(e_1 \to e_2)}$, $D^{(e)}$ are the absorption cross section, scatter cross section, and diffusion coefficient, respectively, for energy group e. These coefficients are constant in each subdomain; absorption and diffusion parameters are shown in Table 1. Cross section values are given in Table 2.

TABLE 2
Scattering coefficients σ_s values for each energy group and each subdomain used for the nonhomogenous problem.

$(e, \hat{e})$	$\mathcal{D}_s$	$\mathcal{D}_a$	$\mathcal{D}_b$
(0,0)	0.134	0.159	0.0396
(0,1)	0.011	0.022	0.026
(0,2)	0.0081	0.052	0.0152
(0,3)	0.0127	0.066	0.0093
(0,4)	0.0148	0.0425	0.0044
(0,5)	0.0107	0.0235	0.0021
(0,6)	0.0054	0.0099	0.00106
(0,7)	0.0022	0.00396	0.00055
(0,8)	0.00076	0.00158	0.000292
(0,9)	0.00026	0.00063	0.000156
(0,10)	0.000144	0.000354	0.00013
(0,11)	2.29e-05	5.7e-05	3.82e-05
(0,12)	3.68e-06	9e-06	1.12e-05
(0,13)	6.1e-07	1.45e-06	3.3e-06
(0,14)	1e-07	2.32e-07	9.7e-07
(0,15)	1.58e-08	3.7e-08	2.85e-07
(0,16)	1.95e-09	4.77e-09	8.4e-08
(0,17)	1.7e-10	4.48e-10	2.39e-08
(0,18)	0.0	0.0	3.05e-10
(0,19)	0.0	0.0	0.0
(1,1)	0.185	0.243	0.057
(1,2)	0.0115	0.0278	0.0374
(1,3)	0.0174	0.0499	0.0177
(1,4)	0.0187	0.0319	0.0105
(1,5)	0.0125	0.0156	0.0057
(1,6)	0.0061	0.0065	0.00302
(1,7)	0.00239	0.00219	0.00162
(1,8)	0.00084	0.00074	0.00086
(1,9)	0.000298	0.000266	0.000465
(1,10)	0.000165	0.000136	0.000387
(1,11)	2.64e-05	1.94e-05	0.000113
(1,12)	4.23e-06	2.88e-06	3.31e-05
(1,13)	7.1e-07	4.42e-07	9.7e-06
(1,14)	1.15e-07	6.9e-08	2.86e-06
(1,15)	1.83e-08	1.06e-08	8.4e-07
(1,16)	2.33e-09	1.67e-09	2.48e-07
(1,17)	2.33e-10	2.06e-10	7.3e-08
(1,18)	0.0	0.0	1.36e-08
(1,19)	0.0	0.0	0.0
(2,2)	0.211	0.397	0.091
(2,3)	0.0171	0.0099	0.053
(2,4)	0.0241	0.0148	0.0266
(2,5)	0.0191	0.0096	0.0145
(2,6)	0.0102	0.0041	0.0079
(2,7)	0.00419	0.00191	0.00427
(2,8)	0.00149	0.00081	0.00232
(2,9)	0.00053	0.000311	0.00126
(2,10)	0.000295	0.000142	0.00106
(2,11)	4.69e-05	1.4e-05	0.000311
(2,12)	7.5e-06	1.24e-06	9.1e-05
(2,13)	1.26e-06	1.11e-07	2.69e-05
(2,14)	2.02e-07	1.04e-08	7.9e-06
(2,15)	3.34e-08	8.9e-10	2.33e-06
(2,16)	4.75e-09	0.0	6.9e-07
(2,17)	4.64e-10	0.0	2.02e-07

$(e, \hat{e})$	$\mathcal{D}_s$	$\mathcal{D}_a$	$\mathcal{D}_b$
(6,6)	0.434	0.442	0.249
(6,7)	0.0185	0.00488	0.205
(6,8)	0.000158	0.0	0.1
(6,9)	4.38e-06	0.0	0.054
(6,10)	5.7e-08	0.0	0.0457
(6,11)	4.98e-09	0.0	0.0134
(6,12)	4.32e-10	0.0	0.00396
(6,13)	0.0	0.0	0.00116
(6,14)	0.0	0.0	0.000342
(6,15)	0.0	0.0	0.000101
(6,16)	0.0	0.0	2.97e-05
(6,17)	0.0	0.0	8.7e-06
(6,18)	0.0	0.0	3.54e-06
(6,19)	0.0	0.0	0.0
(7,7)	0.487	0.517	0.298
(7,8)	0.023	0.0059	0.262
(7,9)	2.57e-05	0.0	0.132
(7,10)	4.86e-06	0.0	0.11
(7,11)	2.14e-07	0.0	0.0325
(7,12)	1.51e-08	0.0	0.0096
(7,13)	1.31e-09	0.0	0.00282
(7,14)	1.14e-10	0.0	0.00083
(7,15)	0.0	0.0	0.000244
(7,16)	0.0	0.0	7.2e-05
(7,17)	0.0	0.0	2.11e-05
(7,18)	0.0	0.0	8.7e-06
(7,19)	0.0	0.0	0.0
(8,8)	0.53	0.618	0.352
(8,9)	0.0193	0.0071	0.322
(8,10)	0.0054	0.0	0.253
(8,11)	0.0	0.0	0.074
(8,12)	0.0	0.0	0.0219
(8,13)	0.0	0.0	0.0065
(8,14)	0.0	0.0	0.0019
(8,15)	0.0	0.0	0.00056
(8,16)	0.0	0.0	0.000164
(8,17)	0.0	0.0	4.84e-05
(8,18)	0.0	0.0	2e-05
(8,19)	0.0	0.0	0.0
(9,9)	0.559	0.6	0.398
(9,10)	0.0074	0.007	0.566
(9,11)	0.00116	0.0	0.161
(9,12)	0.000103	0.0	0.0473
(9,13)	9.1e-06	0.0	0.0139
(9,14)	7.9e-07	0.0	0.0041
(9,15)	6.8e-08	0.0	0.00121
(9,16)	6e-09	0.0	0.000355
(9,17)	5.3e-10	0.0	0.000104
(9,18)	5.8e-11	0.0	4.34e-05
(9,19)	0.0	0.0	0.0
(10,10)	0.541	0.628	0.712
(10,11)	0.00187	0.00256	0.443
(10,12)	0.0	0.0	0.128
(10,13)	0.0	0.0	0.0377
(10,14)	0.0	0.0	0.0111

TABLE 2. *(cont.)*.

$(e,\hat{e})$	$\mathcal{D}_s$	$\mathcal{D}_a$	$\mathcal{D}_b$
(2,18)	0.0	0.0	5.9e-08
(2,19)	0.0	0.0	0.0
(3,3)	0.191	0.312	0.114
(3,4)	0.0229	0.00287	0.081
(3,5)	0.0214	0.0	0.0381
(3,6)	0.0118	0.0	0.0207
(3,7)	0.00436	0.0	0.0112
(3,8)	0.00153	0.0	0.0061
(3,9)	0.00055	0.0	0.00332
(3,10)	0.000301	0.0	0.00278
(3,11)	4.76e-05	0.0	0.00082
(3,12)	7.6e-06	0.0	0.000241
(3,13)	1.28e-06	0.0	7.1e-05
(3,14)	2.03e-07	0.0	2.09e-05
(3,15)	3.38e-08	0.0	6.1e-06
(3,16)	5.4e-09	0.0	1.81e-06
(3,17)	7.3e-10	0.0	5.3e-07
(3,18)	8.4e-11	0.0	1.85e-07
(3,19)	0.0	0.0	0.0
(4,4)	0.232	0.277	0.187
(4,5)	0.0149	0.00258	0.112
(4,6)	0.0097	0.0	0.053
(4,7)	0.0066	0.0	0.0289
(4,8)	0.00261	0.0	0.0157
(4,9)	0.00072	0.0	0.0085
(4,10)	0.000285	0.0	0.0071
(4,11)	2.37e-05	0.0	0.0021
(4,12)	2.16e-06	0.0	0.00062
(4,13)	2.05e-07	0.0	0.000182
(4,14)	2.06e-08	0.0	5.4e-05
(4,15)	2.25e-09	0.0	1.58e-05
(4,16)	1.64e-10	0.0	4.64e-06
(4,17)	0.0	0.0	1.36e-06
(4,18)	0.0	0.0	5.2e-07
(4,19)	0.0	0.0	0.0
(5,5)	0.351	0.257	0.246
(5,6)	0.0138	0.00284	0.168
(5,7)	2.78e-06	0.0	0.073
(5,8)	0.000262	0.0	0.0399
(5,9)	0.000453	0.0	0.0217
(5,10)	0.000197	0.0	0.0182
(5,11)	2.31e-05	0.0	0.0053
(5,12)	2.55e-06	0.0	0.00157
(5,13)	3.8e-07	0.0	0.000463
(5,14)	6.3e-08	0.0	0.000136
(5,15)	6.2e-09	0.0	4.01e-05
(5,16)	5.7e-10	0.0	1.18e-05
(5,17)	7.1e-11	0.0	3.47e-06
(5,18)	0.0	0.0	1.38e-06
(5,19)	0.0	0.0	0.0
(10,15)	0.0	0.0	0.00327
(10,16)	0.0	0.0	0.00096
(10,17)	0.0	0.0	0.000283
(10,18)	0.0	0.0	0.000118
(10,19)	0.0	0.0	7.6e-08
(11,11)	0.527	0.643	0.765
(11,12)	0.00191	0.00262	0.481
(11,13)	0.0	0.0	0.139
(11,14)	0.0	0.0	0.041
(11,15)	0.0	0.0	0.0121
(11,16)	0.0	0.0	0.00355
(11,17)	0.0	0.0	0.00104
(11,18)	0.0	0.0	0.000435
(11,19)	0.0	0.0	8e-07
(12,12)	0.459	0.647	0.783
(12,13)	0.0012	0.00264	0.493
(12,14)	0.0	0.0	0.143
(12,15)	0.0	0.0	0.0421
(12,16)	0.0	0.0	0.0124
(12,17)	0.0	0.0	0.00365
(12,18)	0.0	0.0	0.00152
(12,19)	0.0	0.0	3.37e-06
(13,13)	0.394	0.649	0.789
(13,14)	0.00105	0.00264	0.497
(13,15)	0.0	0.0	0.144
(13,16)	0.0	0.0	0.0425
(13,17)	0.0	0.0	0.0125
(13,18)	0.0	0.0	0.0052
(13,19)	0.0	0.0	1.21e-05
(14,14)	0.44	0.649	0.791
(14,15)	0.00153	0.00264	0.499
(14,16)	0.0	0.0	0.145
(14,17)	0.0	0.0	0.0426
(14,18)	0.0	0.0	0.0177
(14,19)	0.0	0.0	4.18e-05
(15,15)	0.277	0.649	0.791
(15,16)	0.000274	0.00265	0.499
(15,17)	0.0	0.0	0.145
(15,18)	0.0	0.0	0.06
(15,19)	0.0	0.0	0.000143
(16,16)	0.343	0.649	0.792
(16,17)	0.00128	0.00265	0.499
(16,18)	0.0	0.0	0.205
(16,19)	0.0	0.0	0.000487
(17,17)	0.56	0.649	0.794
(17,18)	0.00088	0.00265	0.705
(17,19)	0.0	0.0	0.00166
(18,18)	1.102	0.652	1.717
(18,19)	4.09e-07	1.51e-05	0.00405
(19,19)	0.05	0.693	4.362

7.2. Functions for first and second source moments. We model the source first statistical moment as

$$f^{(e)}(\mathbf{x}) = \begin{cases} \mu^{(e)} & \text{if } \mathbf{x} \in \mathcal{D}_s, \\ 0 & \text{otherwise.} \end{cases} \tag{73}$$

The values of μ are found in Table 1. For the second moment of the source, we use the following function depending on the distance between two points and two energy groups as follows:

$$u^{(e_1 e_2)}(\mathbf{x},\mathbf{y}) = \begin{cases} C_1 \mu^{(e_1)} \mu^{(e_2)} e^{(-\|\mathbf{x}-\mathbf{y}\|_2 - C_2 |\bar{e}_1 - \bar{e}_2|)} + \mu^{(e_1)}\mu^{(e_2)} & \text{if } \mathbf{x} \in \mathcal{D}_s, \\ 0 & \text{otherwise,} \end{cases}$$

where $\bar{e}$ is the medium value of the energy level range of group e, $C_1 = 0.4$, and $C_2 = 100$.

7.3. First moment convergence. Lacking an analytic solution, we measure the error between the discrete solution of each level $L = 1, \ldots, 6$ against an overkill solution obtained for $L = 7$. In Figure 5, each curve represents the error convergence of each energy group. We observe error convergence for all energy groups with upward offsets increasing energy groups. A computed solution is shown in Figure 6, where we plot the sum of energy groups 1–3 as the fast neutron flux, the sum of groups 4–18

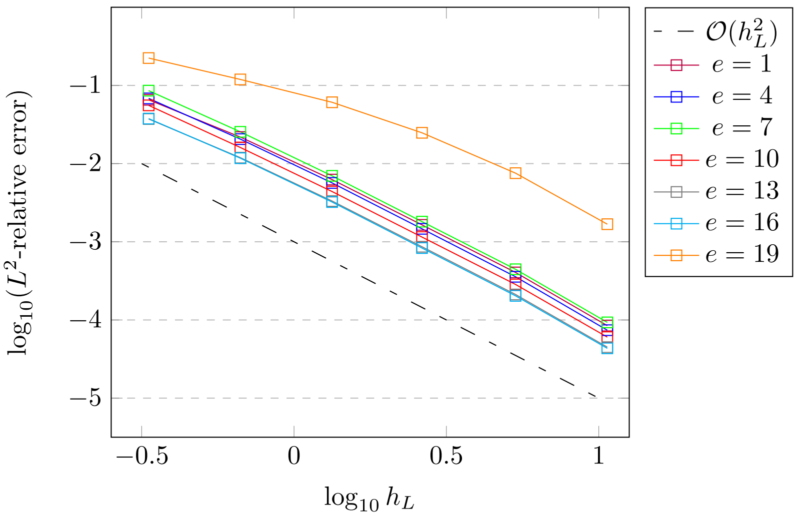

FIG. 5. *Nonhomogeneous problem: L^2-relative error between $u_L^{(e)}(\mathbf{x})$, for $L = 1, \ldots, 6$, and an overkill solution: $u_7^{(e)}(\mathbf{x})$. Convergence of the first energy groups is $\mathcal{O}(h_L^2)$. The last one reaches this convergence order when the mesh is fine enough.*

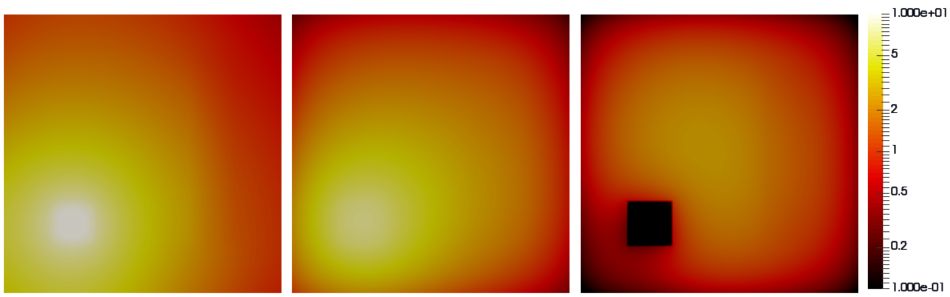

FIG. 6. *Nonhomogeneous problem: u_7 discrete solution for fast solutions (sum of groups 1, 2, 3); epithermal flux (sum of groups 4 to 18); and thermal flux (sum of groups 19 and 20) in logarithmic color scale.*

as the epithermal flux, and the sum of groups 19–20 as the thermal flux. We observe that the fast and epithermal fluxes are concentrated near the source, whereas thermal flux peaks in the region between the lead and the source. The thermal flux in the source region is very small because the source material, Pu-240, is a strong absorber of thermal neutrons. We also observe convergence rates for these combined fluxes in Figure 7.

7.4. Second moment results and convergence. We computed the solution of seven discretization levels for the sparse tensor and five energy groups using full tensor; we compute the error between each level with the highest one: sparse tensor level 7.

The error convergence is shown in Figure 8. In this plot, we can compare the error between sparse tensor and full tensor for each energy group. These results indicate that the sparse tensor method requires fewer degrees of freedom to reach the same

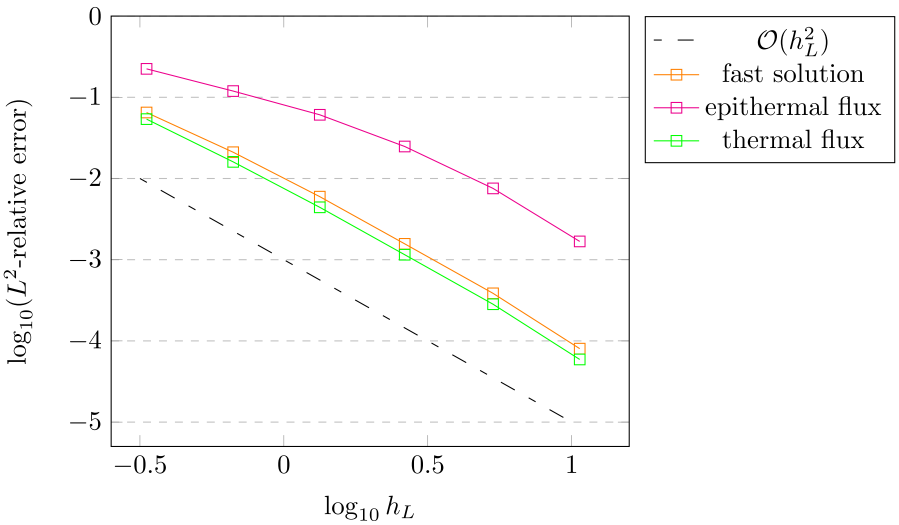

FIG. 7. *Nonhomogeneous problem: L^2-relative errors between discrete approximations at levels $L = 1, \ldots, 6$ for fast, epithermal, and thermal fluxes against those obtained for $L = 7$.*

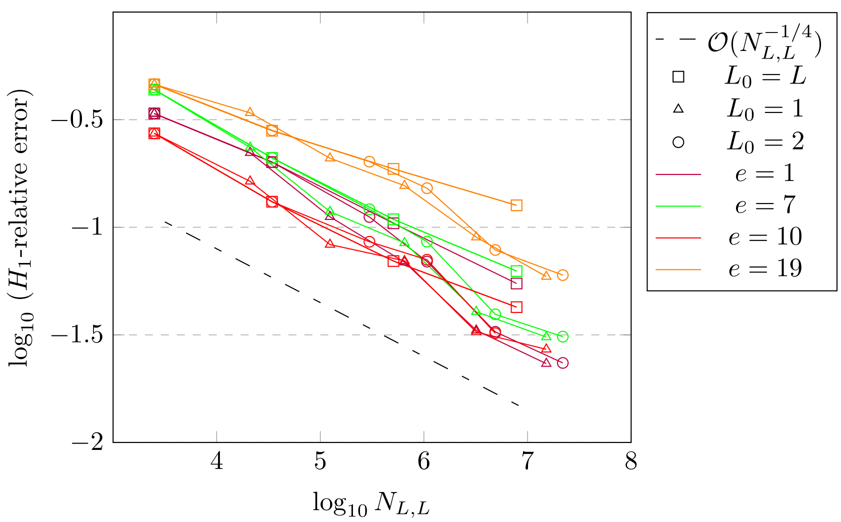

FIG. 8. *Nonhomogeneous case: error convergence plots for sparse and full tensor solutions for the second moment. Convergence of the first energy group using the full tensor is similar to $\mathcal{O}(N_{L,L}^{-1/4})$, which is the same as $\mathcal{O}(h_L)$.*

error level of the full tensor approximation. As in the homogeneous case, convergence rates displayed in Figure 9 appear to be in agreement with those in Proposition 5.16.

We compare the errors obtained by sparse and full tensor approximations against those reached via the MC method. To do this, we generate source samples with a multivariate normal, with source mean and covariance given by the solutions of the first and second moment problems, respectively. The results from 30 different MC simulations are shown in Figure 10. Therein, the results of averaging the solution from different samples are compared against the sparse tensor computation resulting

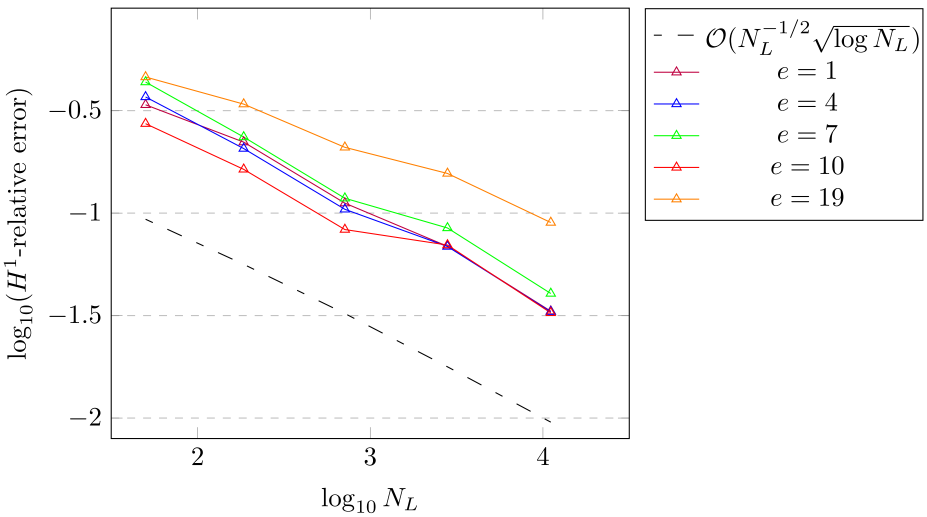

FIG. 9. *Nonhomogeneous case: H^1 relative error between the discrete solution $\widehat{U}^{(ee)}_{L,L_0}(\mathbf{x},\mathbf{x})$ and overkill solution $U^{(ee)}(\mathbf{x},\mathbf{x})$ for $e \in \{1,\dots,4\}$, $L \in \{1,\dots,5\}$. The discrete solution was obtained using a sparse tensor with $L_0 = 1$. The asymptotic error behavior is approximately $\mathcal{O}(N_L^{-1/2}\sqrt{\log N_L})$.*

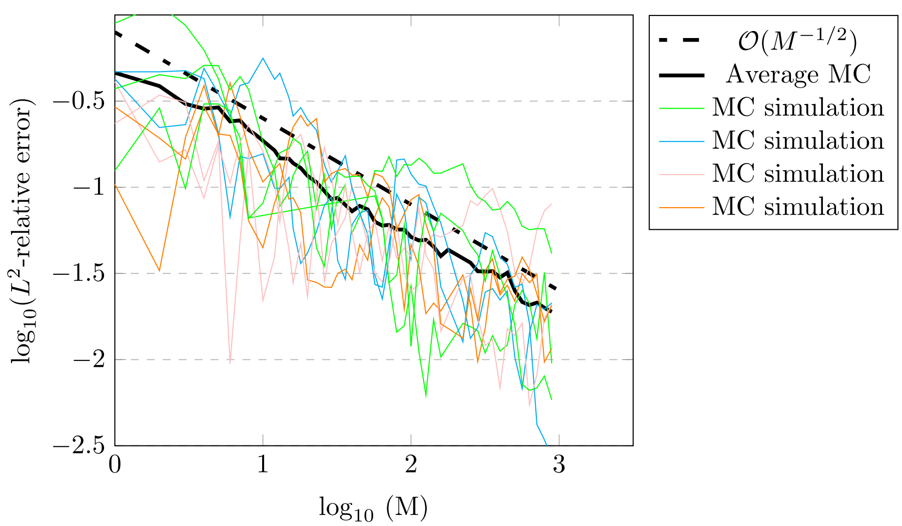

FIG. 10. *Nonhomogenous case: error comparison for an MC simulation of source uncertainty: colored lines represent different MC runs. Each curve shows the error between the average solution until iteration M and $\widehat{U}^{(11)}_{L,L_0}(\mathbf{x},\mathbf{x})$ with $L = 7$ and $L_0 = 2$. The black curve shows the error average of 30 MC runs, which converges with the expected $\mathcal{O}(M^{-1/2})$ rate.*

from considering seven levels. These results indicate that the MC-computed second moment is converging to the deterministic value at a rate of the number of samples raised to the one-half power, as expected.

Figure 11 presents $\mathbb{E}[U_7^{(e_1,e_2)}(\mathbf{x},\mathbf{x})]$ computed using sparse tensor approximations for three different energy groups. We observe that the second moment is largest in the highest energy group inside the source region. However, peak values shift to the

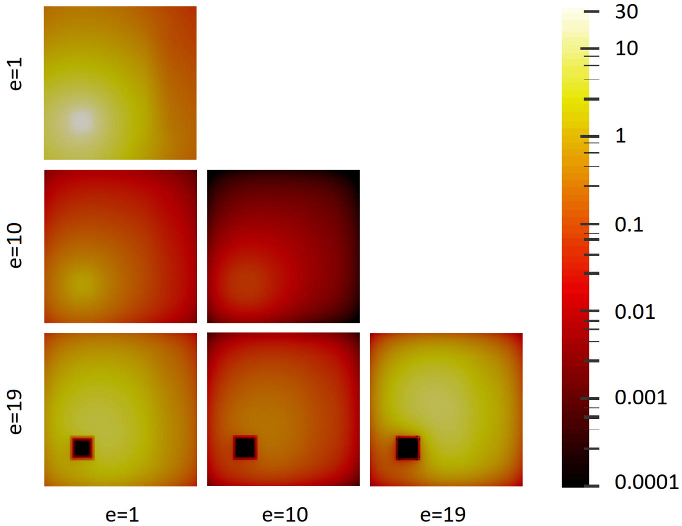

Fig. 11. *Nonhomogenous case:* $\widehat{U}_{L,L_0}^{(e_1 e_2)}(\mathbf{x},\mathbf{x})$ *obtained using the sparse tensor method with* $L = 7$ $L_0 = 2$*. Each plot represents the solution between two different energy groups in logarithmic color scale.*

middle of the domain for low energy groups (in this case, group 19). This is meaningful from a physics perspective as this region is expected to have the most down-scattering due to thermal energies.

8. Conclusions. We have presented an efficient method to quantify the uncertainty in multigroup neutron diffusion problems due to the uncertainties in the source. To achieve this, we took advantage of a sparse tensor finite element formulation to directly and deterministically solve for the first and second moments of the solution. For the examples shown, our spare tensor approximation technique outperformed MC sampling methods and gave accelerated convergence per degree of freedom when compared to the full tensor formulation. Still, more advanced variants of MC such as multilevel MC [1] may be competitive against our method but this is yet to be clarified. We also demonstrated that any energy group forward solving approach employing FEM, even for MC simulations, will be limited by an error constant build-up per energy level. This seems to be of interest by itself and worth further investigation as in our context the double conditioning of the tensor product operators is further enhanced.

There are natural extensions to our work that can be explored in future work. The application of our formulation to eigenvalue problems for nuclear systems is a means to extend the range of possible applications to nuclear criticality safety. We speculate that our technique will work on these problems because in practice they are typically solved using inverse power iteration, where a sequence of fixed source problems are solved to estimate the dominant eigenvalue/eigenvector. The success of such an approach would allow one to incorporate the reportedly large uncertainties in the neutron multiplication rates [4]. Additionally, there are other elliptic problems that could benefit from our treatment, such as conductive heat transfer.

Appendix A. Proof Theorem 5.7. We proceed by induction assuming the case of down-scattering, i.e., $\mathcal{B}^{(\hat{e}e)} \equiv 0$ for $(e,\hat{e}) \in \{1,\dots,N_E\}^2$ with $\hat{e} \geq e$. Galerkin orthogonality between (12) and its discrete counterpart (cf. Problem 5.1) yields

$$\mathsf{a}^{(e)}\left(u^{(e)}-u_h^{(e)}, v_h^{(e)}\right) = -\sum_{\hat{e}=1}^{e-1} \mathsf{b}^{(\hat{e}e)}\left(u^{(\hat{e})}-u_h^{(\hat{e})}, v_h^{(e)}\right) \quad \forall\ v_h^{(e)} \in V_h.$$

Indicating norms and seminorms in $H^s(\mathcal{D})$ solely by the subindex $s \in \mathbb{R}$, and writing down ellipticity and continuity constants of $\mathcal{A}^{(e)}$ as in Proposition 5.6, we derive

$$\begin{aligned} c_1^{\mathcal{A}^{(e)}} \left\|u^{(e)}-u_h^{(e)}\right\|_1^2 &\le \mathsf{a}^{(e)}\left(u^{(e)}-u_h^{(e)}, u^{(e)}-u_h^{(e)}\right) \\ &\le c_2^{\mathcal{A}^{(e)}} \left\|u^{(e)}-u_h^{(e)}\right\|_1 \left\|u^{(e)}-v_h^{(e)}\right\|_1 \\ &\quad + \sum_{\hat{e}=1}^{e-1} c^{(\hat{e}e)} \left\|u^{(\hat{e})}-u_h^{(\hat{e})}\right\|_0 \left\|v_h^{(e)}-u_h^{(e)}\right\|_0, \end{aligned}$$

where $c^{(\hat{e}e)}$ is the continuity constant of the bilinear form $\mathsf{b}^{(\hat{e}e)}$. By the embedding $H^1(\mathcal{D}) \hookrightarrow L^2(\mathcal{D})$ and using the triangle inequality in the second term above, one obtains

$$\left\|u^{(e)}-u_h^{(e)}\right\|_1 \le \frac{c_2^{\mathcal{A}^{(e)}}}{c_1^{\mathcal{A}^{(e)}}} \inf_{v_h^{(e)}\in V_h} \left\|u^{(e)}-v_h^{(e)}\right\|_1 + \frac{2}{c_1^{\mathcal{A}^{(e)}}} \sum_{\hat{e}=1}^{e-1} c^{(e\hat{e})} \left\|u^{(\hat{e})}-u_h^{(\hat{e})}\right\|_0. \tag{74}$$

Let us now consider the case $e = 2$. Since $\mathcal{D}$ is bounded Lipschitz, by Lemma 5.4 and Proposition 5.6, it holds for $\beta \in \{0, 1\}$ and $s \in [\beta, 2]$, that

$$\left\|u^{(2)}-u_h^{(2)}\right\|_\beta \le ch^{s-\beta}\left[\frac{c_2^{\mathcal{A}^{(2)}}}{c_1^{\mathcal{A}^{(2)}}}\left|u^{(2)}\right|_s + \frac{2c_2^{\mathcal{A}^{(1)}}c^{(21)}}{c_1^{\mathcal{A}^{(2)}}c_1^{\mathcal{A}^{(1)}}}\left|u^{(1)}\right|_s\right]$$

with a constant $c > 0$ independent on h. Now, let us assume that, for $e \ge 2$, it holds that

$$\begin{aligned} \left\|u^{(e)}-u_h^{(e)}\right\|_\beta &\le ch^{s-\beta}\frac{c_2^{\mathcal{A}^{(e)}}}{c_1^{\mathcal{A}^{(e)}}}\left|u^{(e)}\right|_s + ch^{s-\beta}\sum_{\hat{e}=1}^{e-2} K^{(e\hat{e})}\left|u^{(\hat{e})}\right|_s \\ &\quad + ch^{s-\beta}\sum_{e'=1}^{e-1} 2^{e-e'}\left(\prod_{\hat{e}=e'}^{e-1}\frac{c^{(\hat{e}+1,\hat{e})}}{c_1^{\mathcal{A}^{(\hat{e}+1)}}}\right)\frac{c_2^{\mathcal{A}^{(e')}}}{c_1^{\mathcal{A}^{e'}}}\left|u^{(e')}\right|_s \end{aligned} \tag{75}$$

for constants $K^{(e\hat{e})} > 0$. We prove this holds for $e+1$ by starting with the general valid statement for any group $e \in \{1, \ldots, N_E\}$:

$$\left\|u^{(e)}-u_h^{(e)}\right\|_\beta \le ch^{s-\beta}\frac{c_2^{\mathcal{A}^{(e)}}}{c_1^{\mathcal{A}^{(e)}}}\left|u^{(e)}\right|_s + \frac{2}{c_1^{\mathcal{A}^{(e)}}}\sum_{\hat{e}=1}^{e-1} c^{(e\hat{e})}\left\|u^{(\hat{e})}-u_h^{(\hat{e})}\right\|_\beta. \tag{76}$$

Then, we can write

(77)

$$\begin{aligned} \left\|u^{(e+1)}-u_h^{(e+1)}\right\|_\beta &\le ch^{s-\beta}\frac{c_2^{\mathcal{A}^{(e+1)}}}{c_1^{\mathcal{A}^{(e+1)}}}\left|u^{(e+1)}\right|_s + \frac{2}{c_1^{\mathcal{A}^{(e+1)}}}\sum_{\hat{e}=1}^{e} c^{(e+1,\hat{e})}\left\|u^{(\hat{e})}-u_h^{(\hat{e})}\right\|_\beta \\ &\le ch^{s-\beta}\frac{c_2^{\mathcal{A}^{(e+1)}}}{c_1^{\mathcal{A}^{(e+1)}}}\left|u^{(e+1)}\right|_s + 2\frac{c^{(e+1,e)}}{c_1^{\mathcal{A}^{(e+1)}}}\left\|u^{(e)}-u_h^{(e)}\right\|_\beta \\ &\quad + \frac{2}{c_1^{\mathcal{A}^{(e+1)}}}\sum_{\hat{e}=1}^{e-1} c^{(e+1,\hat{e})}\left\|u^{(\hat{e})}-u_h^{(\hat{e})}\right\|_\beta. \end{aligned}$$

Using (75), we expand the second term as

$$\begin{aligned}\frac{2c^{(e+1,e)}}{c_1^{\mathcal{A}^{(e+1)}}}\left\|u^{(e)}-u_h^{(e)}\right\|_\beta &\leq ch^{s-\beta}\frac{2c^{(e+1,e)}}{c_1^{\mathcal{A}^{(e+1)}}}\frac{c_2^{\mathcal{A}^{(e)}}}{c_1^{\mathcal{A}^{(e)}}}\left|u^{(e)}\right|_s+ch^{s-\beta}\sum_{\hat{e}=1}^{e-2}\widetilde{K}^{(e\hat{e})}\left|u^{(\hat{e})}\right|_s\\ &\quad+ch^{s-\beta}\frac{c^{(e+1,e)}}{c_1^{\mathcal{A}^{(e+1)}}}\sum_{e'=1}^{e-1}2^{e+1-e'}\left(\prod_{\hat{e}=e'}^{e-1}\frac{c^{(\hat{e}+1,\hat{e})}}{c_1^{\mathcal{A}^{(\hat{e}+1)}}}\right)\frac{c_2^{\mathcal{A}^{(e')}}}{c_1^{\mathcal{A}^{e'}}}\left|u^{(e')}\right|_s\\ &\leq ch^{s-\beta}\left[\sum_{e'=1}^{e}2^{e+1-e'}\left(\prod_{\hat{e}=e'}^{e}\frac{c^{(\hat{e}+1,\hat{e})}}{c_1^{\mathcal{A}^{(\hat{e}+1)}}}\right)\frac{c_2^{\mathcal{A}^{(e')}}}{c_1^{\mathcal{A}^{e'}}}\left|u^{(e')}\right|_s\right.\\ &\quad\left.+\sum_{\hat{e}=1}^{e-2}\widetilde{K}^{(e\hat{e})}\left|u^{(\hat{e})}\right|_s\right]\end{aligned}$$

for new positive constants $\widetilde{K}^{(e\hat{e})}$ using Lemma 5.4 for the last terms. Consequently,

$$\begin{aligned}\left\|u^{(e+1)}-u_h^{(e+1)}\right\|_\beta &\leq ch^{s-\beta}\left[\frac{c_2^{\mathcal{A}^{(e+1)}}}{c_1^{\mathcal{A}^{(e+1)}}}\left|u^{(e+1)}\right|_s+\sum_{\hat{e}=1}^{e-1}\widehat{K}^{(e\hat{e})}\left|u^{(\hat{e})}\right|_s\right.\\ &\quad\left.+\sum_{e'=1}^{e}2^{e+1-e'}\left(\prod_{\hat{e}=e'}^{e}\frac{c^{(\hat{e}+1,\hat{e})}}{c_1^{\mathcal{A}^{(\hat{e}+1)}}}\right)\frac{c_2^{\mathcal{A}^{(e')}}}{c_1^{\mathcal{A}^{e'}}}\left|u^{(e')}\right|_s\right]\end{aligned}\tag{78}$$

again with $\widetilde{K}^{(e\hat{e})}$ positive and independent of h. By induction, (49) is true for any $e\in\{1,\ldots,N_E\}$.

REFERENCES

[1] A. Barth, C. Schwab, and N. Zollinger, *Multi-level Monte Carlo finite element method for elliptic PDEs with stochastic coefficients*, Numer. Math., 119 (2011), pp. 123–161.

[2] K. Beddek, Y. Le Menach, S. Clenet, and O. Moreau, 3-*d stochastic spectral finite-element method in static electromagnetism using vector potential formulation*, IEEE Trans. Magnetics, 47 (2011), pp. 1250–1253.

[3] G. I. Bell and S. Glasstone, *Nuclear Reactor Theory*, Robert E. Kreiger Publishing, Malabar, FL, 1970.

[4] S. R. Bolding, *Simulations of Multiplicity Distributions and Perturbations to Nubar Data*, Tech. Report LA-UR–12-23825, Los Alamos National Laboratory, 2013.

[5] L. Bourhrara, *H*1 *approximations of the neutron transport equation and associated diffusion equations*, Transport Theory Statist. Phys., 35 (2006), pp. 89–108.

[6] T. A. Brunner, T. Mehlhorn, R. G. McClarren, and C. J. Kurecka, *Advances in Radiation Modeling in Alegra: A Final Report for LDRD*-67120*, Efficient Implicit Multigroup Radiation Calculations*, Sandia National Laboratories, 2005.

[7] M. Dashti and A. Stuart, *The Bayesian approach to inverse problems*, in Handbook of Uncertainty Quantification, R. Ghanem et al., eds., Springer, New York, 2016.

[8] Y. Du, Y. Luo, and J.-A. Kong, *Electromagnetic scattering from randomly rough surfaces using the stochastic second-degree method and the sparse matrix/canonical grid algorithm*, IEEE Trans. Geosci. Remote Sensing, 46 (2008), pp. 2831–2839.

[9] S. Duerigen, *Neutron Transport in Hexagonal Reactor Cores Modeled by Trigonal-Geometry Diffusion and Simplified P*3 *Nodal Methods*, Ph.D. thesis, Karlsruhe Institute of Technology, Germany, 2013.

[10] G. J. Habetler and M. A. Martino, *Existence theorems and spectral theory for the multigroup diffusion model*, in Proc. Sympos. Appl. Math. 11, AMS, Providence, RI, 1961, pp. 127–139.

[11] N. H. S. Haidar, *Nodal adjoint method for multigroup diffusion in heterogeneous slab reactors*, Numer. Methods Partial Differential Equations, 8 (1992), pp. 515–535.

[12] M. Hanuš, *Mathematical Modeling of Neutron Transport: Theoretical and Computational Point of View*, Lambert Academic Publishing, 2011.

[13] M. Hanuš and R. G. McClarren, *On the use of symmetrized transport equation in goal-oriented adaptivity*, J. Comput. Theoret. Transp., 45 (2016), pp. 314–333.
[14] H. Harbrecht, *Second moment analysis for robin boundary value problems on random domains*, in Singular Phenomena and Scaling in Mathematical Models, M. Griebel, ed., Springer, New York, 2014, pp. 361–381.
[15] H. Harbrecht, M. Peters, and M. Siebenmorgen, *Combination technique based k-th moment analysis of elliptic problems with random diffusion*, J. Comput. Phys., 252 (2013), pp. 128–141.
[16] H. Harbrecht, R. Schneider, and C. Schwab, *Sparse second moment analysis for elliptic problems in stochastic domains*, Numer. Math., 109 (2008), pp. 385–414.
[17] M. Z. Hasan and R. W. Conn, *A two-dimensional finite element multigroup diffusion theory for neutral atom transport in plasmas*, J. Comput. Phys., 71 (1987), pp. 371–390.
[18] C. D. Hauck and R. G. McClarren, *A collision-based hybrid method for time dependent, linear, kinetic transport equations*, Multiscale Model. Simul., 11 (2013), pp. 1197–1227.
[19] R. Hiptmair, C. Jerez-Hanckes, and C. Schwab, *Sparse tensor edge elements*, BIT, 53 (2013), pp. 925–939.
[20] S. A. Hosseini and F. Saadatian-Derakhshandeh, *Galerkin and generalized least squares finite element: A comparative study for multi-group diffusion solvers*, Progr. Nuclear Energy, 85 (2015), pp. 473–490.
[21] C. Jerez-Hanckes and C. Schwab, *Electromagnetic wave scattering by random surfaces: uncertainty quantification via sparse tensor boundary elements*, IMA J. Numer. Anal., 37 (2017), pp. 1175–1210.
[22] P. Knupp and K. Salari, *Verification of Computer Codes in Computational Science and Engineering*, CRC Press, Boca Raton, FL, 2002.
[23] J. R. Lamarsh, *Introduction to Nuclear Reactor Theory*, 3rd ed., Pearson, London, 2001.
[24] C. Lingus, *Analytical test cases for neutron and radiation transport codes*, in proceedings of the Second Conference on Transport Theory, 1971, p. 655.
[25] R. G. McClarren, *Computational Nuclear Engineering and Radiological Science Using Python*, Academic Press, New York, 2017.
[26] R. G. McClarren, *Uncertainty Quantification and Predictive Computational Science: A Foundation for Physical Scientists and Engineers*, Springer, New York, 2018.
[27] R. G. McClarren, R. P. Drake, J. E. Morel, and J. P. Holloway, *Theory of radiative shocks in the mixed, optically thick-thin case*, Phys. Plasmas, 17 (2010), 093301.
[28] R. G. McClarren and R. B. Lowrie, *Manufactured solutions for the $P1$ radiation-hydrodynamics equations*, J. Quant. Spectroscopy Radiative Transfer, 109 (2008), pp. 2590–2602.
[29] R. G. McClarren, D. Ryu, and R. P. Drake, *A physics informed emulator for laser-driven radiating shock simulations*, Reliability Engineering System Safety, 96 (2010), pp. 1194–1207.
[30] R. G. McClarren and J. G. Wohlbier, *Analytic solutions for ion-electron-radiation coupling with radiation and electron diffusion*, J. Quant. Spectroscopy Radiative Transfer, 112 (2010), pp. 119–130.
[31] R. B. Myneni and G. Asrar, *Radiative transfer in three-dimensional atmosphere-vegetation media*, J. Quant. Spectroscopy, 49 (1993), pp. 585–598.
[32] R. Sanchez and N. J. McCormick, *A review of neutron transport approximations*, Nuclear Sci. Engrg., 80 (1982), pp. 481–535.
[33] P. Saracco, S. Dulla, and P. Ravetto, *On the spectrum of the multigroup diffusion equations*, Progr. Nuclear Energy, 59 (2012), pp. 86–95.
[34] C. Schwab, E. Süli, and R. A. Todor, *Sparse finite element approximation of high-dimensional transport-dominated diffusion problems*, M2AN Math. Model. Numer. Anal., 42 (2008), pp. 777–819.
[35] C. Schwab and R. A. Todor, *Karhunen-Loève approximation of random fields by generalized fast multipole methods*, J. Comput. Phys., 217 (2006), pp. 100–122.
[36] W. Stacey, *Nuclear Reactor Physics*, John Wiley & Sons, New York, 2007.
[37] O. Steinbach, *Numerical Approximation Methods for Elliptic Boundary Value Problems: Finite and Boundary Elements*, Texts in Appl. Math., Springer New York, 2007.
[38] H. Stewart, *Properties of Solutions and Eigenfunctions of Multigroup Diffusion Problems*, Tech. Report 2048, Institut für Neutronenphysik und Reaktortechnik, 1974.
[39] H. Stewart, *Spectral theory of heterogeneous diffusion systems*, J. Math. Anal. Appl., 54 (1976), pp. 59–78.
[40] T. von Petersdorff and C. Schwab, *Sparse finite element methods for operator equations with stochastic data*, Appl. Math., 51 (2006), pp. 145–180.

[41] Y. Wang and J. Ragusa, *Application of hp adaptivity to the multigroup diffusion equations*, Nuclear Sci. Engrg., 161 (2009), pp. 22–48.

[42] W. Zwermann, A. Aures, L. Gallner, V. Hannstein, B. Krzykacz-Hausmann, K. Velkov, and J. Martinez, *Nuclear data uncertainty and sensitivity analysis with XSUSA for fuel assembly depletion calculations*, Nuclear Engrg. Technol., 46 (2014), pp. 343–352.